
Improving TabPFN’s Synthetic Data Generation by Integrating Causal Structure

Davide Tugnoli*¹

Andrea De Lorenzo†²

Marco Virgolin‡³

Giovanni Cinià§⁴

¹Department of Mathematics, Informatics and Geosciences, University of Trieste, Trieste, Italy

²Department of Engineering and Architecture, University of Trieste, Trieste, Italy

³InSilicoTrials Technologies BV, The Netherlands

⁴Medical Informatics Dept., Amsterdam UMC, Institute for Logic, Language and Computation, University of Amsterdam, The Netherlands

Abstract

Synthetic tabular data generation addresses data scarcity and privacy constraints in a variety of domains. Tabular Prior-Data Fitted Network (TabPFN), a recent foundation model for tabular data, has been shown capable of generating high-quality synthetic tabular data. However, TabPFN is autoregressive: features are generated sequentially by conditioning on the previous ones, depending on the order in which they appear in the input data. We demonstrate that when the feature order conflicts with causal structure, the model produces spurious correlations that impair its ability to generate synthetic data and preserve causal effects. We address this limitation by integrating causal structure into TabPFN’s generation process through two complementary approaches: Directed Acyclic Graph (DAG)-aware conditioning, which samples each variable given its causal parents, and a Completed Partially Directed Acyclic Graph (CPDAG)-based strategy for scenarios with partial causal knowledge. We evaluate these approaches on controlled benchmarks and six CSuite datasets, assessing structural fidelity, distributional alignment, privacy preservation, and Average Treatment Effect (ATE) preservation. Across most settings, DAG-aware conditioning improves the quality and stability of synthetic data relative to vanilla TabPFN. The CPDAG-based strategy shows moderate improvements, with effectiveness depending on the number of oriented edges. These results indicate that injecting causal structure into autoregressive generation enhances the reliability of synthetic tabular data.

1 INTRODUCTION

Synthetic tabular data generation is becoming an important approach to handle data scarcity and privacy concerns in many domains [Shi et al., 2025b]. This is especially relevant in fields such as healthcare, finance, and policy research, where privacy regulations and ethical constraints often limit access to real data. In pharmaceutical research, for example, synthetic data can be used to simulate drug effects for safety and efficacy, while protecting patient confidentiality. For tabular data, generation methods must avoid producing close copies of training samples, especially when data is limited.

However, generating reliable synthetic tabular data is challenging because real datasets usually contain complex causal relations among variables. Generation methods that ignore such dependencies may create spurious correlations that differ from the true data-generating process. When synthetic data are used to augment limited real data or simulate clinical scenarios, misleading dependencies can propagate to treatment effect estimates. In drug development, for instance, inaccurate estimation of treatment effects from flawed synthetic data could lead to costly trials on ineffective drugs or the exclusion of promising ones.

Recent foundation models for tabular data, such as Tabular Prior-Data Fitted Network (TabPFN) [Hollmann et al., 2025], have shown promising results by pre-training on millions of synthetic datasets derived from Structural Causal Models (SCMs) [Pearl, 2009]. Pre-training on such diverse datasets is particularly valuable when real data are limited, a common scenario in domains like healthcare. This advantage becomes even more important for synthetic data generation, which requires predicting all features rather than a single target variable as in traditional classification or regression tasks. Extensions of TabPFN¹ enable unsupervised, autoregressive generation of synthetic tabular data. However, TabPFN’s autoregressive approach generates variables

*davide.tugnoli@phd.units.it

†andrea.delorenzo@units.it

‡marco.virgolin@gmail.com

§g.cina@amsterdamumc.nl

¹<https://github.com/PriorLabs/tabpfn-extensions>

sequentially without explicitly accounting for causal structure. Although the model averages predictions over random permutations of the conditioning set, this mitigates but does not eliminate order sensitivity: during generation, each variable can only condition on features that appear earlier in the sequence. When the generation order conflicts with causal dependencies, particularly in the presence of colliders, the model may introduce spurious correlations that compromise the reliability of synthetic data.

This work studies the autoregressive nature of TabPFN-based synthetic data generation, identifies a fundamental limitation, and proposes methods to address it. Our contributions are as follows:

1. We demonstrate that TabPFN synthetic data quality depends heavily on the order of the features in the input data due to the absence of causal reasoning, with this sensitivity persisting even at large training sizes.
2. We propose causal conditioning strategies that leverage known or discovered causal structure, showing improvements for both full Directed Acyclic Graph (DAG) knowledge and partial Completed Partially Directed Acyclic Graph (CPDAG) information, when sufficiently oriented, across distributional quality metrics.
3. We quantify how synthetic data errors propagate to treatment effect preservation, demonstrating substantial misestimation that could lead to incorrect decisions in applications such as drug development.

All code, datasets, and detailed numerical results are publicly available.²

2 RELATED WORK

Generative approaches to synthetic tabular data range from classical statistical methods to deep models based on Generative Adversarial Networks (GANs), Variational Autoencoders (VAEs), diffusion models, and autoregressive architectures [Shi et al., 2025b].

Early deep generative models adapted architectures from image generation. TGAN [Xu and Veeramachaneni, 2018] applied GANs to mixed continuous–categorical tables using Long Short-Term Memory-based generation, while CTGAN [Xu et al., 2019] addressed class imbalance and multimodal distributions. CTAB-GAN [Zhao et al., 2021] further improved semantic fidelity. More recently, diffusion models have achieved strong performance [Kotelnikov et al., 2023, Zhang et al., 2024, Shi et al., 2025a]. While effective for statistical fidelity, these methods generate all features simultaneously without explicit causal structure.

Autoregressive approaches factorize the joint distribution into sequential conditionals $p(x_j | x_{C(j)})$, where $C(j)$ denotes the conditioning set. Early work used Classification And Regression Trees (CART) to generate features sequentially [Reiter, 2005]. GReaT treats tabular rows as text sequences for language model generation [Borisov et al., 2023]. TabularARGN [Tiwald et al., 2025] randomizes feature orderings during training to learn conditionals across different subsets. Among foundation models, TabPFN [Hollmann et al., 2023, 2025] achieves state-of-the-art performance on small datasets via in-context learning. Pre-trained on millions of synthetic datasets sampled from SCMs, it acquired strong inductive biases without requiring retraining on target data. TabPFGen extends TabPFN to generative tasks via energy-based sampling rather than autoregressive conditioning [Ma et al., 2024], but neither approach explicitly conditions on causal graphs during generation.

Causal approaches integrate structural knowledge directly into generation. DECAF embeds SCMs into the architecture for interventional debiasing [Van Breugel et al., 2021]. Causal-TGAN structures its generator according to a causal graph [Wen et al., 2022]. DATGAN incorporates expert DAGs to enforce structural dependencies [Lederrey et al., 2022]. CA-GAN combines causal discovery with reinforcement learning [Nguyen et al., 2025]. Unlike TabPFN, these models are trained from scratch per dataset and explicitly use DAG structure to guide generation.

Recent work has applied transformer-based meta-learning to causal effect estimation. Do-PFN [Robertson et al., 2025] adapts the PFN framework to predict conditional interventional distributions from observational data, taking covariates and treatment as input. CausalPFN [Balazadeh et al., 2025] trains a transformer on a causal prior to estimate expected potential outcomes, also conditioning on covariates and treatment. Both models predict outcomes under intervention but do not model the full joint distribution over all variables. MACE-TNP [Dhir et al., 2025] addresses a related task, estimating Bayesian model-averaged interventional distributions from observational data via neural processes; it similarly targets interventional queries rather than joint density modeling. To our knowledge, this is the first work to combine a foundation model with explicit causal structure for synthetic tabular data generation, addressing autoregressive ordering violations and collider bias through DAG-aware and CPDAG-based conditioning strategies.

3 METHODOLOGY

3.1 TABPFN CAUSAL EXTENSIONS

TabPFN is a transformer-based model pre-trained on approximately 130 million synthetic datasets, each sampled from a randomly generated SCM with diverse graph structures, functional relationships, and noise distributions [Hollmann

²<https://github.com/DavideTugnoli/tabpfn-causal-synthetic>

et al., 2025]. At inference time, it receives an entire dataset as context and produces predictions in a single forward pass via in-context learning, without retraining on the target data. For synthetic data generation, the model is applied autoregressively: features are generated sequentially following the column order of the input data. Denoting this ordering as π , each feature $x_{\pi(i)}$ at position i in the sequence is sampled from a conditional distribution

$$p(x_{\pi(i)} \mid \mathcal{C}(\pi(i))), \quad (1)$$

where the conditioning context $\mathcal{C}(\pi(i)) = \{x_{\pi(0)}, \dots, x_{\pi(i-1)}\}$ consists of all features preceding position i in the ordering. When no context is available ($i = 0$), the model conditions on random noise to approximate the marginal distribution.

Hollmann et al. [2025] recognize that the autoregressive nature induces a specific bias due to the local ordering of variables within the conditioning set $\mathcal{C}(\pi(i))$. To mitigate this issue, they propose averaging predictions over multiple random permutations of the conditioning set at inference time. However, this averaging strategy does not address the limitation imposed by the global ordering π . When π does not respect the causal structure, the model may still condition on descendant variables when generating their ancestors, inducing spurious correlations.

For instance, consider a collider structure $X \rightarrow Z \leftarrow Y$, where the causes X and Y are marginally independent. If the global ordering places the common effect Z before its parents, the model may e.g. generate X conditioned on Z , then Y conditioned on both Z and X . Conditioning on the collider Z makes X and Y conditionally dependent; generating sequentially from these learned conditionals propagates this dependence to the marginal distribution of the synthetic data, introducing spurious correlations.

To address this limitation, we introduce causal conditioning strategies that align TabPFN’s generative process with known or partially known causal structures. Causal relationships between variables can be formally represented using a DAG $\mathcal{G} = (V, E)$, where nodes V correspond to variables and directed edges E indicate direct causal influences [Pearl, 2009]. When such a graph is available, we condition each variable only on its causal parents rather than on all previously generated features:

$$\mathcal{C}_{\text{DAG}}(x_{\pi(i)}) = \{x_j : x_j \rightarrow x_{\pi(i)} \text{ in } \mathcal{G}\}. \quad (2)$$

Variables are generated following a topological ordering of \mathcal{G} , ensuring that all parents have been generated before each child.³

³A topological ordering alone does not imply DAG-aware conditioning: the vanilla strategy of Eq. (1) can also follow a topological ordering, but conditions on all predecessors rather than on causal parents only.

However, in most real-world scenarios, the true causal graph is unknown. While causal discovery algorithms attempt to reconstruct the DAG from data, they often recover only partial information, identifying some edge orientations while leaving others ambiguous. This partial knowledge can be represented by a CPDAG \mathcal{G}^* [Chickering, 2002], which includes directed edges where the orientation is uniquely determined and undirected edges where multiple orientations remain compatible with the data.

Due to the partially directed structure of a CPDAG, Equation (2) cannot be readily applied. We define a generation ordering σ that places variables with known causal parents before the remaining ones, and propose the following hybrid conditioning strategy:

$$\mathcal{C}(x_{\sigma(i)}) = \begin{cases} \text{pa}_{\mathcal{G}^*}(x_{\sigma(i)}) & \text{if fully directed,} \\ \{x_{\sigma(0)}, \dots, x_{\sigma(i-1)}\} & \text{otherwise,} \end{cases} \quad (3)$$

where “fully directed” means that $x_{\sigma(i)}$ has at least one directed adjacent edge and no undirected adjacent edges in \mathcal{G}^* . Variables satisfying this condition are generated according to their causal parents, while the rest revert to sequential conditioning on all predecessors in the ordering. When every edge in the CPDAG is directed, Eq. (3) recovers the conditioning set of Eq. (2) for all non-isolated variables; when no edge is directed, it reduces to the conditioning set of Eq. (1).

4 EXPERIMENTAL DESIGN

4.1 EVALUATION METRICS AND CONTROLS

We evaluate synthetic data quality using three metrics widely adopted in benchmark frameworks such as SynthEval [Lautrup et al., 2025] and the Differential Privacy Synthetic Data Challenge organized by the National Institute of Standards and Technology [Ridgeway et al., 2021], capturing complementary requirements: structural dependency, pairwise fidelity, and privacy. The Correlation Matrix Difference (CMD) quantifies how well the overall dependency structure among variables is preserved. We compute mixed correlation matrices combining Cramér’s V for categorical–categorical pairs, the correlation ratio η for categorical–numerical pairs, and Spearman’s rank correlation for numerical–numerical pairs. We replace Pearson (the SynthEval default) with Spearman to capture monotonic relationships in datasets with nonlinear dependencies. The metric is computed as the Frobenius norm of the difference between real and synthetic correlation matrices, i.e., $\text{CMD} = \|C_{\text{real}} - C_{\text{synthetic}}\|_F$.

The k -Marginal Total Variation Distance (kMTVD) with $k = 2$ measures pairwise distributional fidelity. Continuous variables are discretized into $B = 20$ quantile-based bins. For two empirical distributions P and Q , the total variation

distance is $\text{TVD} = \frac{1}{2} \sum_x |P(x) - Q(x)|$, and the metric is the mean Total Variation Distance (TVD) across all variable pairs.

The Nearest-Neighbor Adversarial Accuracy (NNAA) [Yale et al., 2020] assesses privacy preservation by quantifying the distinguishability between synthetic and real data based on nearest-neighbor distances. We use SynthEval’s implementation with the Gower distance. For each real sample i , the distance $d_{TS}(i)$ to its nearest synthetic neighbor is compared with the distance $d_{TT}(i)$ to its nearest real neighbor. Similarly, for each synthetic sample j , the distance $d_{ST}(j)$ to its nearest real neighbor is compared with the distance $d_{SS}(j)$ to its nearest synthetic neighbor. The adversarial accuracy is

$$\text{NNAA} = \frac{1}{2} \left[\frac{1}{n} \sum_{i=1}^n \mathbf{1}(d_{TS}(i) > d_{TT}(i)) + \frac{1}{n} \sum_{j=1}^n \mathbf{1}(d_{ST}(j) > d_{SS}(j)) \right], \quad (4)$$

where $\mathbf{1}(\cdot)$ denotes the indicator function, and n is the number of samples in both the real and synthetic datasets. Values near 0.5 indicate that synthetic and real data are hard to distinguish.

We assess the statistical significance of differences between conditioning strategies using the Wilcoxon signed-rank test with Pratt’s method for handling tied observations, applying Holm correction for prespecified comparisons. Effect sizes are quantified using the Hodges–Lehmann estimator, the median of pairwise averages of differences [Hodges Jr and Lehmann, 2011].

4.2 DATASETS

We conduct experiments on three dataset classes, ranging from fully controlled hand-crafted settings to public benchmark datasets and realistic clinical scenarios.

4.2.1 Custom Collider SCM

We design a four-variable SCM containing a collider to evaluate TabPFN’s sensitivity to causal structure under fully controlled conditions. Colliders (variables with multiple parent edges) pose a fundamental challenge for autoregressive generators because they induce conditional dependencies between otherwise independent variables.

The DAG of this SCM is defined as $X_0 \rightarrow X_1 \leftarrow X_2 \leftarrow X_3$, where X_1 is the collider node. Although X_0 and X_2 are marginally independent ($X_0 \perp\!\!\!\perp X_2$), conditioning on their common child X_1 induces dependence between them ($X_0 \not\perp\!\!\!\perp X_2 \mid X_1$). When an autoregressive generator conditions on X_1 while generating its parents, it correctly learns

that X_0 and X_2 are dependent given X_1 . However, sequential sampling from these conditionals propagates this dependence into the marginal distribution, creating spurious marginal correlation between variables that should be independent. We construct the SCM with near-deterministic linear relationships to amplify this collider bias effect and enable clear detection of spurious associations introduced by inappropriate conditioning strategies. Full structural equations appear in Appendix A.

4.2.2 CSuite Benchmark Datasets

Next, we consider the Microsoft CSuite benchmark [Geffner et al., 2024], a collection of hand-crafted SCMs designed for evaluating causal discovery and inference under known ground-truth graphs.

We select six datasets with at least four nodes and distinct structures, covering a range of causal scenarios: CSuite Non-linear Simpson (CNS), CSuite Symprod Simpson (CSS), and CSuite Mixed Simpson (CMS) (four nodes each, variants of Simpson’s paradox with continuous or mixed-type variables), CSuite Mixed Confounding (CMC) (twelve nodes, mixed data types and complex confounding structures), CSuite Large Backdoor (CLB) and CSuite Weak Arrows (CWA) (nine nodes each, large topologies with backdoor paths and weak causal effects). Each dataset includes predefined intervention specifications for treatment effect estimation.

4.2.3 Simglucose Type 1 Diabetes Mellitus Simulator

Finally, we evaluate on a realistic dataset derived from the UVA/Padova Type 1 Diabetes Mellitus (T1DM) Simulator⁴ [Man et al., 2009], a Food and Drug Administration (FDA)-approved model of glucose-insulin dynamics. The original simulator integrates a system of ordinary differential equations over time. Following the approach in [Esponera and Cinà, 2025], we use an acyclic reformulation and adapt it to a static setting by removing temporal dependencies.

The dataset contains 38 variables, including physiological states, patient-specific parameters, and exogenous actions. Although the physiological equations define a clear causal progression among the endogenous states, the relations among patient-specific parameters are not known, i.e., we do not know the full DAG. These parameters are sampled from distributions based on clinical data and represent heterogeneous virtual patients. Because only partial causal knowledge is available, we use this dataset to test whether partial topological ordering still improves generation quality.

⁴<https://github.com/jxx123/simglucose.git>

4.3 EXPERIMENTS ON SYNTHETIC DATA QUALITY

To ensure reproducibility, we conduct all experiments using the official implementation of TabPFN (version 2.1.0). We compare three conditioning strategies to assess how causal structure affects synthetic data quality: *vanilla* TabPFN (which conditions sequentially on predecessors, Equation (1)), DAG-aware generation (which conditions on causal parents), and CPDAG-based generation (which combines directed and undirected causal relationships). We conduct experiments on the Custom SCM (CSM), the six CSuite benchmark datasets, and SimGlucose (SGL), using the default value of 3 permutations for the internal averaging mechanism described in Section 3.1.

To assess robustness across different data availability scenarios, we test multiple training sizes $N \in \{20, 50, 100, 200, 500\}$ ⁵ with 100 resampling iterations per configuration. We strictly separate training and test data by creating fixed test sets of 2000 samples for each dataset. For the CSM and SGL, we generate 6000 samples total, select test samples once using a fixed random seed, and sample training data from the remaining 4000 samples. For CSuite benchmarks, we use the predefined test sets and sample training data from the remaining pool.

To study the susceptibility of TabPFN-based data generation to the input ordering, we evaluate three column orderings: *original ordering* (as provided in the dataset, or a random permutation if it coincides with topological or reverse topological), *topological ordering* (parents before children), and *reverse topological ordering* (children before parents), which maximizes causal violations, illustrating a potential worst-case scenario.

For CPDAG-based generation, we test both *discovered* CPDAGs, learned from the training data via the order-independent Peter-Clark (PC)-stable algorithm ($\alpha = 0.05$) [Colombo et al., 2014], and *minimal* CPDAGs, constructed by orienting only the V-structures from the true DAG while leaving other edges undirected. For the custom SCM, we apply the Fisher-Z conditional independence test to assess edge dependencies within the PC algorithm. For CSuite datasets with categorical or mixed-type variables, we use a hybrid strategy: Kernel Conditional Independence (KCI) test for continuous pairs, G^2 test for discrete pairs, and k -Nearest Neighbors Conditional Mutual Information (k -NN CMI) ($k = 5, 500$ permutations) for mixed pairs. For all strategies, we generate synthetic datasets of the same size as the test sets and evaluate them using CMD, kMTVD, and NNAA.

⁵ N denotes the number of samples provided to TabPFN as in-context learning data.

4.4 EXPERIMENTS ON TREATMENT EFFECT PRESERVATION

We evaluate how well synthetic data preserve causal effects by measuring Average Treatment Effect (ATE) preservation. This addresses a practical scenario: given a small interventional dataset (e.g., from a pilot trial), we generate synthetic data and assess whether the treatment effect is preserved.

For all datasets, we construct fixed balanced test sets by sampling equally from both intervention arms with a fixed random seed, using generated interventional data for CSM and SGL and benchmark-provided data for CSuite.

We test training sizes $N \in \{20, 50, 100, 200, 500, 1000\}$ with 100 resampling iterations per configuration, extending to larger sizes as effect estimation generally benefits from more samples. For each training size, we construct the training set by combining equal numbers of samples from both intervention arms into a single dataset, which is then provided to TabPFN as in-context data.

The ground truth ATE on the test set is computed as $ATE_{\text{test}} = \mathbb{E}[Y \mid \text{do}(X = x_1)] - \mathbb{E}[Y \mid \text{do}(X = x_0)]$, where x_1 and x_0 denote the two prespecified intervention values and Y the predefined outcome variable for each dataset. Synthetic data are then generated using the three conditioning strategies, and the corresponding ATE on the synthetic data is computed as $ATE_{\text{synthetic}} = \mathbb{E}[\hat{Y} \mid \text{do}(X = x_1)] - \mathbb{E}[\hat{Y} \mid \text{do}(X = x_0)]$, where the expectation here is taken over the synthetic data. Our evaluation metric is the absolute ATE difference, $\Delta_{\text{ATE}} = |ATE_{\text{test}} - ATE_{\text{synthetic}}|$. Lower values indicate better preservation of causal effects. In comparative analyses, we test whether one method produces significantly lower absolute errors than another.

5 RESULTS

5.1 EXPERIMENTS ON SYNTHETIC DATA QUALITY

5.1.1 Topological Column Ordering Improves Vanilla TabPFN

Vanilla TabPFN is sensitive to feature ordering across all datasets, with sensitivity decreasing at larger training sizes (Figure A1). Topological ordering yields significant improvements in CMD for 26 out of 40 combinations of dataset and train size (Figure 1), with three degradations on CSS at training sizes $N \leq 100$. Datasets CSM and SGL show the greatest improvements in CMD: largest at small training sizes for CSM, and increasing with training size for SGL. The kMTVD and NNAA results confirm these trends (Figure A2). Table A1 reports correlation coefficients for variable pairs that should be independent in CSM, confirming that vanilla TabPFN introduces spurious correlations up

to $|\rho| \approx 0.15$ while DAG-aware generation does not.

Conversely, reverse topological ordering predominantly degrades performance across metrics (Appendix E). This confirms that column ordering significantly impacts TabPFN’s data generation quality.

5.1.2 DAG-Aware Generation Outperforms Vanilla TabPFN

DAG-aware generation shows significant improvements in CMD for 24 of 35 configurations (Figure 2, left), compared to vanilla TabPFN with original ordering, with two degradations on CSS at $N = 20$ and $N = 100$. Improvements are strongest on CSM, CWA, and CMC, with improvement sizes decreasing at larger training sizes. The kMTVD and NNAA results also show widespread improvements across datasets (Figure A5), with one degradation on CLB in kMTVD.

Comparing vanilla TabPFN and DAG-aware generation under the same topological ordering isolates the contribution of causal conditioning from the choice of feature ordering. Across all three metrics, DAG-aware generation shows consistent improvements with minimal degradations (Appendix G).

5.1.3 CPDAG-Based Generation Shows Improvements Compared to Vanilla TabPFN When Sufficiently Oriented

The minimal CPDAG shows 15 significant improvements and 3 significant degradations in CMD (Figure 2, right). Two degradations occur on CLB (at $N = 20$ and $N = 50$), and one on CSS (at $N = 20$). The discovered CPDAG shows no significant improvements and 4 significant degradations in CMD (Figure A8). Three of the four degradations occur on CMC, where PC orients most discovered edges with low accuracy (Table A2). Most configurations (31 of 35) show no significant difference from vanilla TabPFN. The kMTVD and NNAA results confirm these patterns (Figures A9 and A10).

5.2 EXPERIMENTS ON TREATMENT EFFECT PRESERVATION

5.2.1 Vanilla TabPFN with Topological Ordering Improves ATE Preservation

Topological ordering yields 18 significant improvements in ATE preservation across 42 configurations (Figure 3), with 2 degradations, one on CMC and one on CSS, at 20 samples. CSM shows the greatest improvements, particularly at smaller training sizes. On SGL, topological ordering produces 5 significant improvements out of 6 training sizes (Figure A11), with larger effect sizes than other datasets.

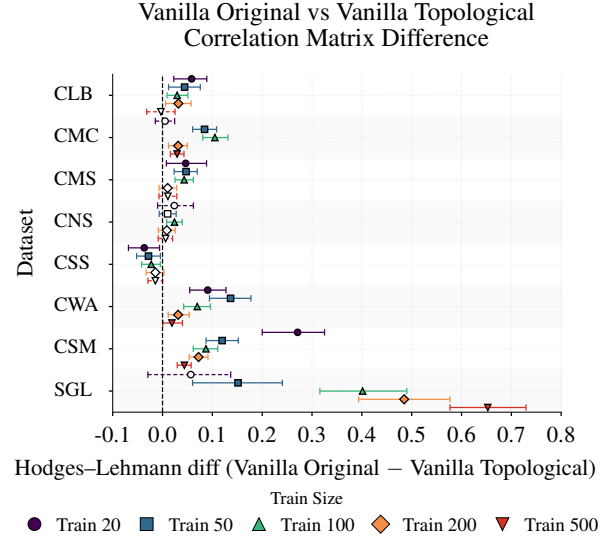


Figure 1: Hodges–Lehmann estimates comparing vanilla TabPFN with original ordering versus topological ordering in CMD. Positive values indicate that topological ordering achieves lower metric values (i.e., better synthetic data quality). Filled markers with solid error bars indicate significance at $p < 0.05$ (Holm correction).

Reverse topological ordering produces large degradations on CSM (Figure A12).

5.2.2 DAG-Aware Generation Improves ATE Preservation

DAG-aware generation shows 26 significant improvements across 42 configurations with 2 degradations, one on CMC and one on CSS, at 20 samples (Figure 4, left), compared to 18 improvements for vanilla topological ordering. CSM and CMS show significant improvements across all training sizes, with the largest reductions at 20 samples. CNS shows significant improvements at most training sizes. Results for direct comparison using the same topological ordering appear in Figure A13.

5.2.3 Minimal CPDAG Improves ATE Preservation

The minimal CPDAG shows 23 significant improvements across 42 configurations, with one degradation on CMC at $N = 20$ and one on CSS at $N = 200$ (Figure 4, right).

Improvements are strongest on CNS (across all training sizes), CMS and CSM (at smaller training sizes). The discovered CPDAG shows no consistent effects, with one improvement and one degradation across 42 configurations (Figure A14 and Table A3).

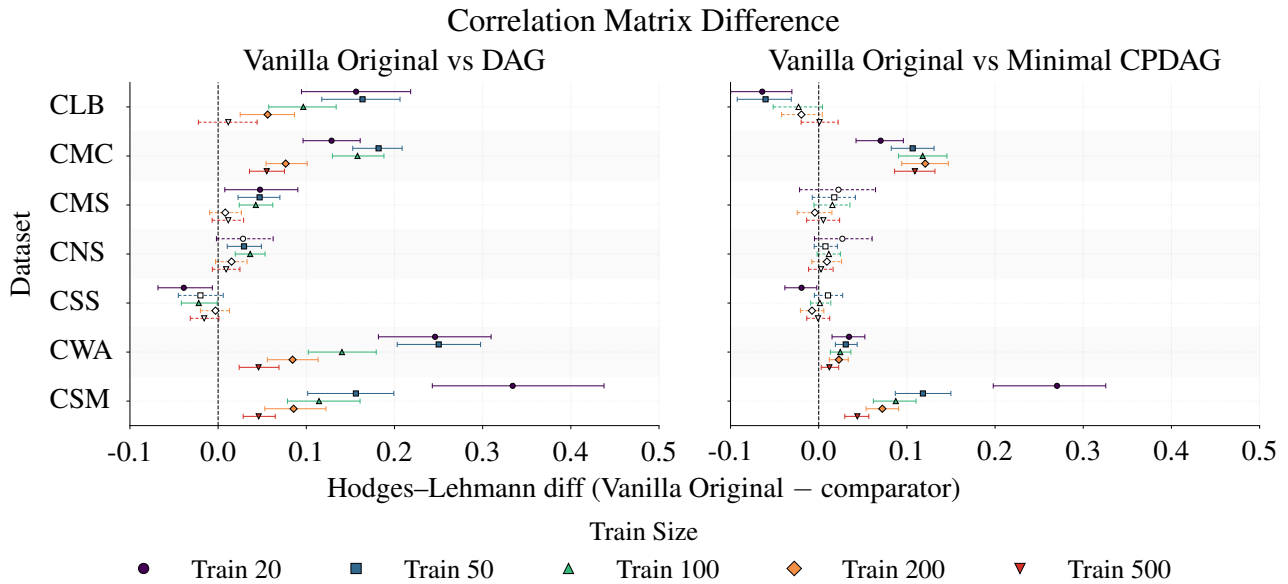


Figure 2: Hodges–Lehmann estimates comparing vanilla TabPFN with original ordering versus DAG-aware generation (left) and versus minimal CPDAG (right) in CMD. Positive values indicate that the respective method achieves lower metric values (i.e., better synthetic data quality). Filled markers with solid error bars indicate significance at $p < 0.05$ (Holm correction).

6 DISCUSSION

Vanilla TabPFN is sensitive to feature order during generation. When features do not follow causal dependencies, the model conditions on descendants while generating ancestors, inducing spurious correlations. Reordering columns topologically improves both distribution quality and treatment effect preservation, while reversing causal direction worsens both. DAG-aware generation conditions each variable only on its causal parents rather than on all previously generated features; this produces higher-quality synthetic data with minimal degradations across datasets and metrics. The single degradation in kMTVD occurs on CLB, whose sparse causal structure (most nodes have a single parent) limits the conditioning context available to the model.

When the complete DAG is unknown, partial causal information can still help. Minimal CPDAGs orienting only V-structures show improvements in synthetic data quality and ATE preservation. However, CPDAGs discovered from data often leave many edges unoriented, causing the model to fall back to vanilla sequential conditioning; when the recovered graph is sufficiently inaccurate, they can even degrade performance. Effective causal conditioning requires sufficient edge orientation in the partial graph, and the position of V-structures within the causal graph also matters. When these are central (as in CMC), generating oriented variables first allows the remaining variables to follow the causal direction, producing improvements. When they are at the end of a causal chain (as in CLB), generating oriented variables first effectively reverses the generation order

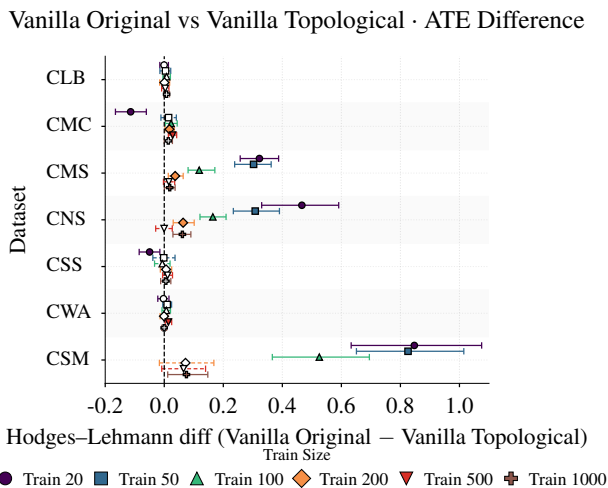


Figure 3: Hodges–Lehmann estimates of the reduction in absolute ATE error (Δ_{ATE}) when comparing vanilla TabPFN with original ordering versus topological ordering on CSuite and CSM datasets. Positive values indicate that topological ordering produces smaller errors (closer to ground truth), while negative values indicate larger errors. Filled markers with solid error bars indicate significance at $p < 0.05$ (Holm correction).

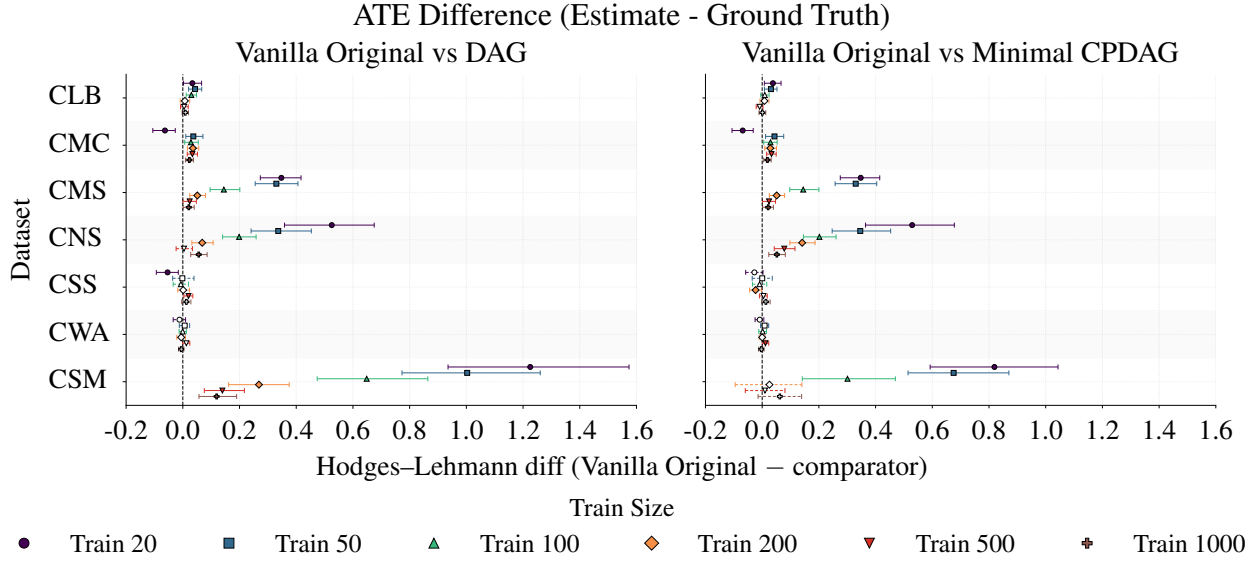


Figure 4: Hodges–Lehmann estimates of the reduction in absolute ATE error (Δ_{ATE}) when comparing vanilla TabPFN with original ordering versus DAG-aware generation (left) and versus minimal CPDAG (right) on ATE preservation. Positive values indicate that the respective method (DAG-aware or CPDAG-based) produces smaller errors (closer to ground truth), while negative values indicate larger errors. Filled markers with solid error bars indicate significance at $p < 0.05$ (Holm correction).

relative to the causal direction, leading to degradations.

Causal conditioning preserves causal effects better than vanilla TabPFN, particularly with limited training data. On CSM, DAG-aware generation reduces absolute ATE error by approximately 1.23 units at 20 samples compared to vanilla TabPFN, with improvements persisting at larger training sizes. Since the CSM uses near-deterministic relationships ($\sigma = 10^{-5}$), we verify that these findings hold under higher noise ($\sigma = 10^{-2}$): results confirm that the benefits of causal conditioning extend beyond the near-deterministic regime (Appendix M). The degradation on CMC at $N = 20$ in the ATE experiments also occurs with vanilla TabPFN under topological ordering, which does not modify the generation mechanism. This indicates that the effect is a property of the model under this input configuration rather than a consequence of causal conditioning.

Our findings extend to realistic datasets with incomplete causal knowledge. The SGL dataset, derived from an FDA-approved T1DM simulator with 38 variables and partial causal information, shows improvements in synthetic data quality under partial topological ordering (Figure 1). Unlike the other datasets, these improvements increase with training size, which we attribute to the interplay between sample size and data dimensionality: with 38 variables, the model needs sufficient context to benefit from correct ordering. In the smaller SCMs (4 to 12 variables), the model already benefits from correct ordering at small N , but this advantage diminishes as data increases. This highlights relevance for

real-world medical applications, where accurate treatment effect preservation from synthetic data can support early-stage research while protecting patient privacy.

6.1 LIMITATIONS AND FUTURE WORK

This work is subject to the following limitations. First, DAG-aware generation assumes full knowledge of the causal structure, which is rarely available in practice. CPDAG-based generation shows that partial causal information can still be valuable, but its effectiveness depends on V-structure placement in ways that cannot be predicted without knowledge of the true graph. Second, causal discovery relied solely on PC-stable. A preliminary evaluation with REX [Renero et al., 2026], which returns fully oriented DAGs, yielded worse synthetic data quality since incorrect orientations propagate into the conditioning strategy (Appendix N). Third, CMD assumes monotonic dependencies and is uninformative for SCMs with multiplicative equations, as in CSS. Fourth, the interventional analysis focused exclusively on the ATE; other causal estimands or downstream tasks may respond differently to causal conditioning. Finally, our study focused primarily on TabPFN. Future work should explore ordering strategies for incomplete causal knowledge, evaluate a broader range of causal discovery algorithms, select evaluation metrics based on dependency structure, and test these findings on other neural autoregressive architectures, such as TabularARGN [Tiwald et al., 2025].

References

- Vahid Balazadeh, Hamidreza Kamkari, Valentin Thomas, Junwei Ma, Bingru Li, Jesse C Cresswell, and Rahul Krishnan. Causalpfn: Amortized causal effect estimation via in-context learning. In *The Thirty-ninth Annual Conference on Neural Information Processing Systems*, 2025.
- Vadim Borisov, Kathrin Seßler, Tobias Leemann, Martin Pawelczyk, and Gjergji Kasneci. Language models are realistic tabular data generators. In *The Eleventh International Conference on Learning Representations*, 2023.
- David Maxwell Chickering. Optimal structure identification with greedy search. *Journal of Machine Learning Research*, 3:507–554, 2002.
- Diego Colombo, Marloes H Maathuis, et al. Order-independent constraint-based causal structure learning. *J. Mach. Learn. Res.*, 15(1):3741–3782, 2014.
- Anish Dhir, Cristiana Diaconu, Valentinian Mihai Lungu, James Requeima, Richard E Turner, and Mark van der Wilk. Estimating interventional distributions with uncertain causal graphs through meta-learning. In *The Thirty-ninth Annual Conference on Neural Information Processing Systems*, 2025.
- Ana Esponera and Giovanni Cinà. Inducing causal structure applied to glucose prediction for t1dm patients. In Biwei Huang and Mathias Drton, editors, *Proceedings of the Fourth Conference on Causal Learning and Reasoning*, volume 275 of *Proceedings of Machine Learning Research*, pages 920–946. PMLR, May 2025. URL <https://proceedings.mlr.press/v275/esponera25a.html>. 07–09 May.
- Tomas Geffner, Javier Antoran, Adam Foster, Wenbo Gong, Chao Ma, Emre Kiciman, Amit Sharma, Angus Lamb, Martin Kukla, Nick Pawlowski, et al. Deep end-to-end causal inference. *Transactions on Machine Learning Research*, 2024.
- Joseph L Hodges Jr and Erich L Lehmann. Estimates of location based on rank tests. In *Selected works of EL Lehmann*, pages 287–300. Springer, 2011.
- Noah Hollmann, Samuel Müller, Katharina Eggenberger, and Frank Hutter. TabPFN: A transformer that solves small tabular classification problems in a second. In *The Eleventh International Conference on Learning Representations*, 2023.
- Noah Hollmann, Samuel Müller, Lennart Purucker, Arjun Krishnakumar, Max Körfer, Shi Bin Hoo, Robin Tibor Schirrmester, and Frank Hutter. Accurate predictions on small data with a tabular foundation model. *Nature*, 637(8045):319–326, 2025.
- Akim Kotelnikov, Dmitry Baranchuk, Ivan Rubachev, and Artem Babenko. Tabddpm: Modelling tabular data with diffusion models. In *International conference on machine learning*, pages 17564–17579. PMLR, 2023.
- Anton D Lauthrup, Tobias Hyrup, Arthur Zimek, and Peter Schneider-Kamp. Syntheval: a framework for detailed utility and privacy evaluation of tabular synthetic data. *Data Mining and Knowledge Discovery*, 39(1):6, 2025.
- Gael Lederrey, Tim Hillel, and Michel Bierlaire. Datgan: Integrating expert knowledge into deep learning for synthetic tabular data. *arXiv preprint arXiv:2203.03489*, 2022.
- Junwei Ma, Apoorv Dankar, George Stein, Guangwei Yu, and Anthony Caterini. Tabpfn—tabular data generation with tabpfn. *arXiv preprint arXiv:2406.05216*, 2024.
- Chiara Dalla Man, Marc D. Breton, and Claudio Cobelli. Physical activity into the meal glucose—insulin model of type 1 diabetes: In silico studies. *Journal of Diabetes Science and Technology*, 3(1):56–67, 2009. doi: 10.1177/193229680900300107. URL <https://doi.org/10.1177/193229680900300107>. PMID: 20046650.
- Tu Anh Hoang Nguyen, Dang Nguyen, Tri-Nhan Vo, Thuc Duy Le, and Sunil Gupta. Causal-aware generative adversarial networks with reinforcement learning. *arXiv preprint arXiv:2510.24046*, 2025.
- Judea Pearl. *Causality: Models, Reasoning, and Inference*. Cambridge University Press, Cambridge, UK, 2nd edition, 2009. ISBN 978-0521895606.
- Jerome P Reiter. Using cart to generate partially synthetic public use microdata. *Journal of official statistics*, 21(3): 441, 2005.
- Jesús Renero, Roberto Maestre, and Idoia Ochoa. Rex: Causal discovery based on machine learning and explainability techniques. *Pattern Recognition*, 172:112491, 2026.
- Diane Ridgeway, Mary F Theofanos, Terese W Manley, and Christine Task. Challenge design and lessons learned from the 2018 differential privacy challenges, 2021.
- Jake Robertson, Arik Reuter, Siyuan Guo, Noah Hollmann, Frank Hutter, and Bernhard Schölkopf. Do-pfn: In-context learning for causal effect estimation. In *The Thirty-ninth Annual Conference on Neural Information Processing Systems*, 2025.
- Juntong Shi, Minkai Xu, Harper Hua, Hengrui Zhang, Stefano Ermon, and Jure Leskovec. Tabdiff: a mixed-type diffusion model for tabular data generation. In *The Thirteenth International Conference on Learning Representations*, 2025a.

- Ruxue Shi, Yili Wang, Mengnan Du, Xu Shen, Yi Chang, and Xin Wang. A comprehensive survey of synthetic tabular data generation. *arXiv preprint arXiv:2504.16506*, 2025b.
- Paul Tiwald, Ivona Krchova, Andrey Sidorenko, Mariana Vargas Vieyra, Mario Scriminaci, and Michael Platzer. Tabularargn: A flexible and efficient auto-regressive framework for generating high-fidelity synthetic data. *arXiv preprint arXiv:2501.12012*, 2025.
- Boris Van Breugel, Trent Kyono, Jeroen Berrevoets, and Mihaela Van der Schaar. Decaf: Generating fair synthetic data using causally-aware generative networks. *Advances in Neural Information Processing Systems*, 34:22221–22233, 2021.
- Bingyang Wen, Yupeng Cao, Fan Yang, Koduvayur Subbalakshmi, and Rajarathnam Chandramouli. Causal-TGAN: Modeling tabular data using causally-aware GAN. In *ICLR 2022 Workshop on Deep Generative Models for Highly Structured Data*, 2022.
- Lei Xu and Kalyan Veeramachaneni. Synthesizing tabular data using generative adversarial networks. *arXiv preprint arXiv:1811.11264*, 2018.
- Lei Xu, Maria Skoularidou, Alfredo Cuesta-Infante, and Kalyan Veeramachaneni. Modeling tabular data using conditional gan. *Advances in neural information processing systems*, 32, 2019.
- Andrew Yale, Saloni Dash, Ritik Dutta, Isabelle Guyon, Adrien Pavao, and Kristin P Bennett. Generation and evaluation of privacy preserving synthetic health data. *Neurocomputing*, 416:244–255, 2020.
- Hengrui Zhang, Jiani Zhang, Zhengyuan Shen, Balasubramaniam Srinivasan, Xiao Qin, Christos Faloutsos, Huzefa Rangwala, and George Karypis. Mixed-type tabular data synthesis with score-based diffusion in latent space. In *The Twelfth International Conference on Learning Representations*, 2024.
- Zilong Zhao, Aditya Kunar, Robert Birke, and Lydia Y Chen. Ctab-gan: Effective table data synthesizing. In *Asian conference on machine learning*, pages 97–112. PMLR, 2021.

Improving TabPFN’s Synthetic Data Generation by Integrating Causal Structure

(Supplementary Material)

A CUSTOM SCM DEFINITION

The custom collider SCM has causal structure $X_3 \rightarrow X_2 \rightarrow X_1 \leftarrow X_0$, with structural equations:

$$X_0 \sim \mathcal{N}(0, 1) \tag{5}$$

$$X_3 \sim \mathcal{N}(0, 1) \tag{6}$$

$$X_2 = 0.5 X_3 + \epsilon_2, \quad \epsilon_2 \sim \mathcal{N}(0, \sigma^2) \tag{7}$$

$$X_1 = 5.0 X_0 + 10.0 X_2 + \epsilon_1, \quad \epsilon_1 \sim \mathcal{N}(0, \sigma^2) \tag{8}$$

where $\sigma = 10^{-5}$. Variables X_0 and X_3 are independent root nodes, and X_0 and X_2 are d-separated since X_2 depends only on X_3 .

B ORDER SENSITIVITY ACROSS DATASETS

To quantify how much feature ordering affects synthetic data quality, we measure the variability of each metric across the three orderings (original, topological, reverse topological).

For each dataset and training size, we compute:

- The metric value under each of the three orderings
- The range: maximum value minus minimum value
- Bootstrap confidence intervals for the median range (1000 resamples, $\alpha = 0.05$)

A large range indicates that the model is highly sensitive to feature ordering. A small range indicates consistent performance regardless of ordering.

Figure A1 shows results for CMC. This dataset exemplifies a general pattern observed across all evaluated datasets: ordering sensitivity decreases with training size but persists even at larger sample sizes. Results for additional datasets are available in the code repository.

C VANILLA TABPFN WITH TOPOLOGICAL ORDERING RESULTS

Figure A2 reports kMTVD and NNAA results for vanilla TabPFN with topological ordering. In kMTVD, topological ordering yields 30 significant improvements and 1 degradation on CLB at 500 samples (left panel). In NNAA, it yields 27 significant improvements with no degradations (right panel).

D SPURIOUS CORRELATIONS IN CUSTOM SCM

Table A1 reports Pearson correlation coefficients for variable pairs that should be independent according to the custom SCM causal structure (Appendix A). The test set baseline confirms the expected independence with correlations close to zero ($\rho \approx 0.02$). We report results for $N \in \{20, 100, 500\}$; intermediate training sizes ($N = 50, 200$) exhibit the same monotonic pattern and are available in the code repository. Vanilla TabPFN with original and reverse topological orderings introduces substantial spurious correlations, particularly at small training sizes ($|\rho| \approx 0.15$ at $N = 20$). DAG-aware generation maintains near-zero correlations across all training sizes. Minimal CPDAG performs similarly to vanilla topological, while discovered CPDAG behaves like vanilla original, reflecting how undirected edges are resolved based on column order.

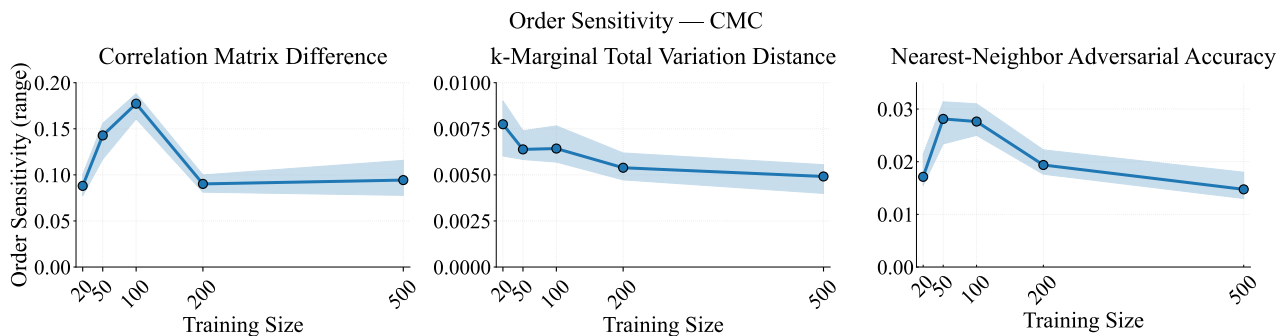


Figure A1: Order sensitivity for vanilla TabPFN on CMC. Y-axis shows the range of CMD (left), kMTVD ($k = 2$, center), and NNAA (right) values across three feature orderings: original, topological, and reverse topological. Shaded regions show 95 % bootstrap confidence intervals.

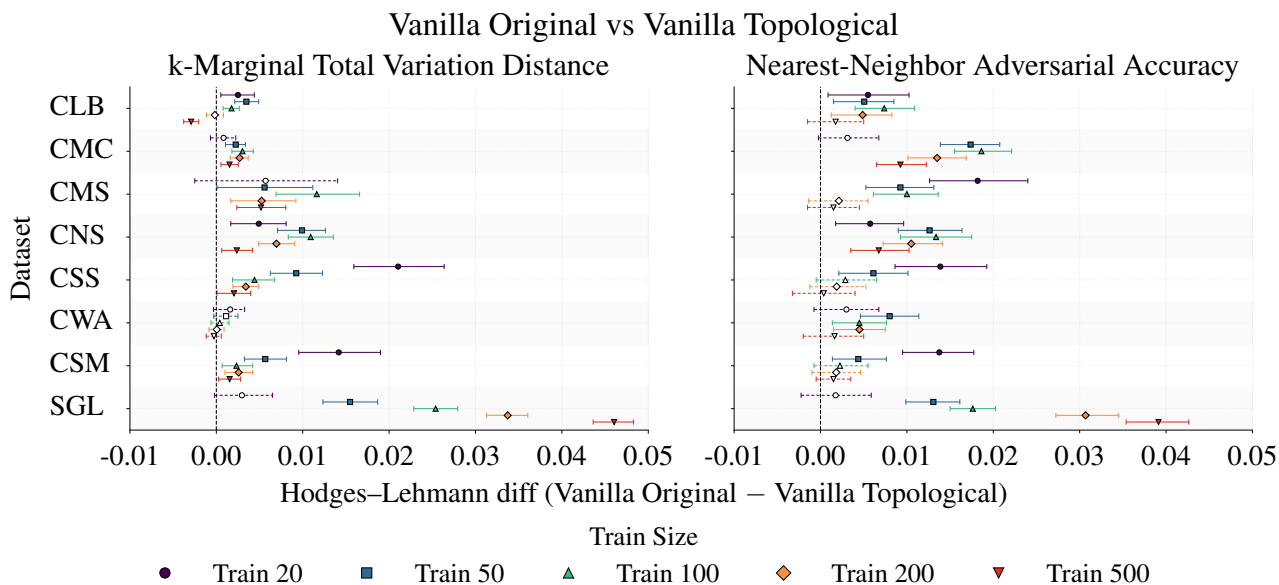


Figure A2: Hodges–Lehmann estimates comparing vanilla TabPFN with original ordering versus topological ordering in kMTVD ($k = 2$, left) and NNAA (right). Positive values indicate that topological ordering achieves lower metric values (i.e., better synthetic data quality). Filled markers with solid error bars indicate significance at $p < 0.05$ (Holm correction).

Table A1: Mean Pearson correlation coefficients for independent variable pairs in the custom collider SCM. Values close to zero indicate correct independence preservation. Standard deviations across 100 repetitions in parentheses.

Method	$\rho(X_0, X_3)$	$\rho(X_0, X_2)$
<i>Train size N = 20</i>		
Vanilla original	-0.149 (0.203)	-0.150 (0.202)
Vanilla topological	-0.018 (0.110)	-0.018 (0.109)
Vanilla reverse top.	-0.127 (0.195)	-0.123 (0.197)
DAG-aware	0.004 (0.021)	0.004 (0.021)
Minimal CPDAG	-0.018 (0.109)	-0.018 (0.110)
Discovered CPDAG	-0.150 (0.202)	-0.151 (0.201)
<i>Train size N = 100</i>		
Vanilla original	-0.042 (0.114)	-0.043 (0.114)
Vanilla topological	-0.017 (0.064)	-0.017 (0.063)
Vanilla reverse top.	-0.047 (0.101)	-0.045 (0.101)
DAG-aware	0.000 (0.020)	0.000 (0.020)
Minimal CPDAG	-0.017 (0.063)	-0.017 (0.064)
Discovered CPDAG	-0.043 (0.113)	-0.043 (0.114)
<i>Train size N = 500</i>		
Vanilla original	-0.028 (0.043)	-0.028 (0.043)
Vanilla topological	-0.003 (0.025)	-0.003 (0.025)
Vanilla reverse top.	-0.033 (0.040)	-0.032 (0.040)
DAG-aware	0.001 (0.023)	0.001 (0.023)
Minimal CPDAG	-0.003 (0.025)	-0.003 (0.025)
Discovered CPDAG	-0.028 (0.043)	-0.028 (0.043)
Test set	0.022 -	0.022 -

E VANILLA TABPFN WITH REVERSE TOPOLOGICAL ORDERING RESULTS

This section reports results for vanilla TabPFN with reverse topological ordering. Reverse topological ordering shows predominantly negative effects across metrics, with 4 significant degradations in CMD and 17 in kMTVD (Figure A3, left and right, respectively), against 4 significant improvements in CMD and 1 in kMTVD. NNAA confirms this pattern with 10 significant degradations and 1 significant improvement (Figure A4).

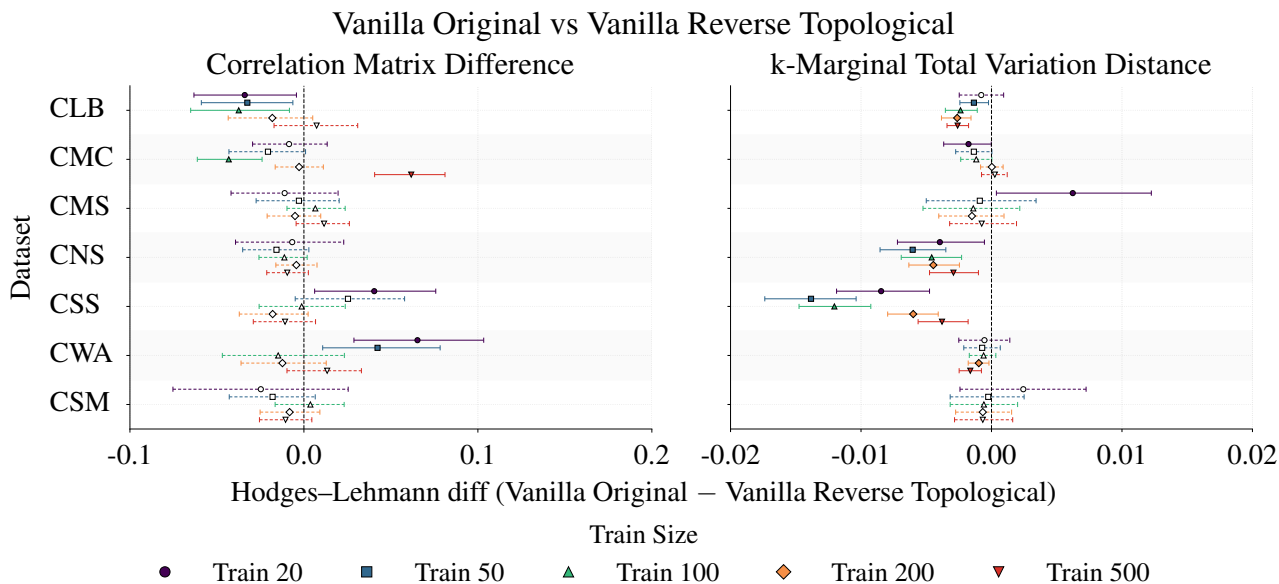


Figure A3: Hodges–Lehmann estimates comparing vanilla TabPFN with original ordering versus reverse topological ordering in CMD (left) and kMTVD ($k = 2$, right). Positive values indicate that reverse topological ordering achieves lower metric values (i.e., better synthetic data quality). Filled markers with solid error bars indicate significance at $p < 0.05$ (Holm correction).

F DAG-AWARE GENERATION VS VANILLA: kMTVD AND NNAA RESULTS

Figure A5 reports kMTVD and NNAA results comparing vanilla TabPFN with original ordering versus DAG-aware generation. In kMTVD, DAG-aware generation yields 30 significant improvements and 1 degradation on CLB at 500 samples (left panel). In NNAA, it yields 29 significant improvements with no degradations (right panel).

G DAG-AWARE GENERATION WITH TOPOLOGICAL ORDERING

We compare DAG-aware generation and vanilla TabPFN when both use topological ordering, isolating the contribution of causal parent-based conditioning from the feature ordering itself.

DAG-aware generation shows 20 significant improvements with no degradations in CMD, 10 improvements and 2 degradations in kMTVD, and 14 improvements and 1 degradation in NNAA (Figures A6 and A7).

H CPDAG-BASED GENERATION: CMD, kMTVD, AND NNAA RESULTS

Figure A8 reports CMD results for discovered CPDAG, showing 4 degradations with no improvements. Results for minimal CPDAG in CMD appear in Figure 2. Figure A9 reports kMTVD results for CPDAG-based generation. In kMTVD, minimal CPDAG shows 19 significant improvements and 4 degradations, all on CLB; discovered CPDAG shows 1 improvement and 4 degradations. The single improvement occurs on CMS at $N = 500$, where PC orients 52% of discovered edges with 0.67 direction precision (Table A2). Three of the four degradations occur on CMC, where PC orients most discovered edges with

Vanilla Original vs Vanilla Reverse Topological · Nearest-Neighbor Adversarial Accuracy

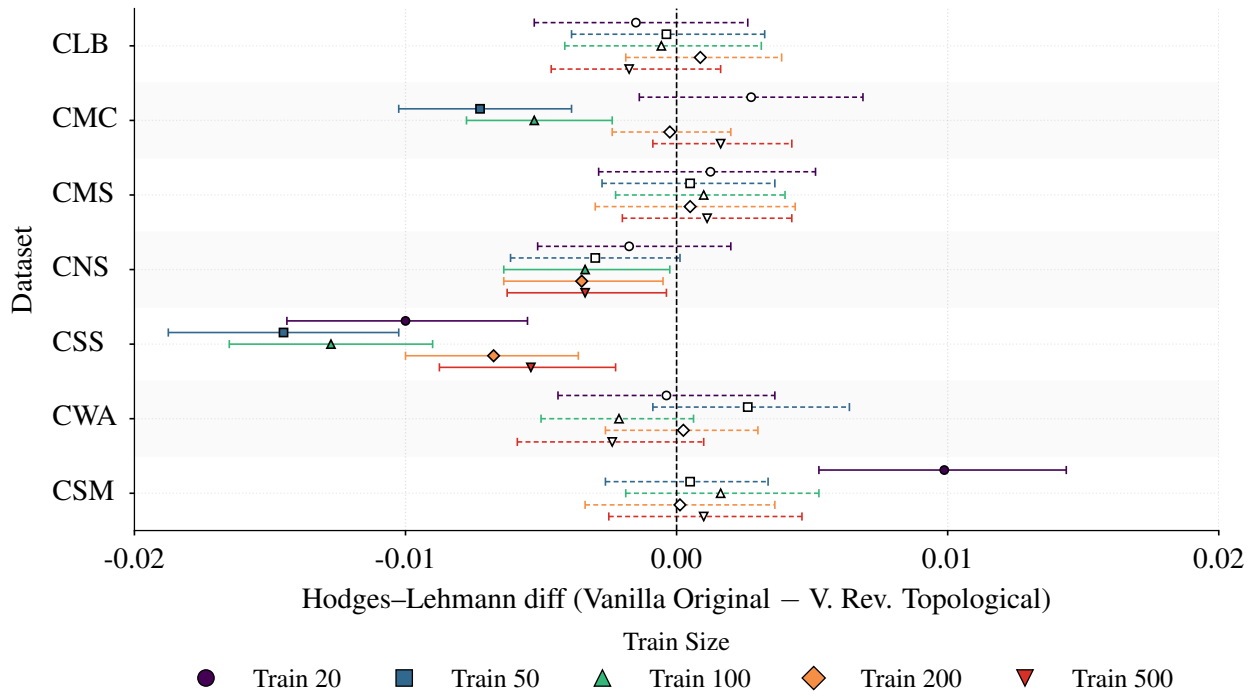


Figure A4: Hodges–Lehmann estimates comparing vanilla TabPFN with original ordering versus reverse topological ordering in NNAA. Positive values indicate that reverse topological ordering achieves lower metric values (i.e., better synthetic data quality). Filled markers with solid error bars indicate significance at $p < 0.05$ (Holm correction).

Vanilla Original vs DAG

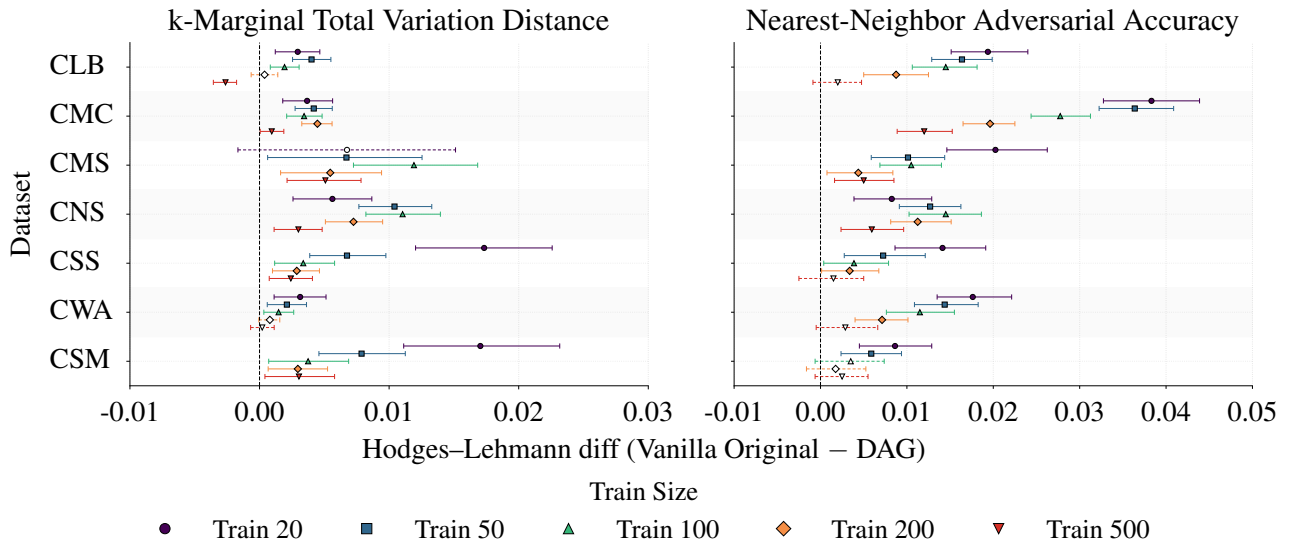


Figure A5: Hodges–Lehmann estimates comparing vanilla TabPFN with original ordering versus DAG-aware generation in kMTVD ($k = 2$, left) and NNAA (right). Positive values indicate that DAG-aware generation achieves lower metric values (i.e., better synthetic data quality). Filled markers with solid error bars indicate significance at $p < 0.05$ (Holm correction).

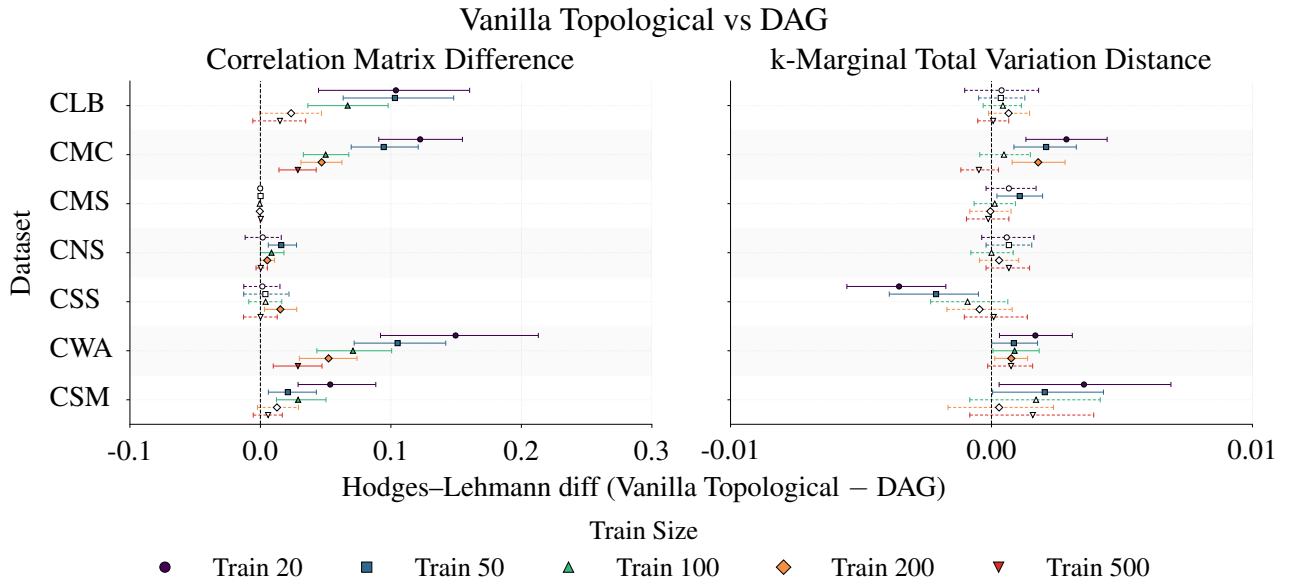


Figure A6: Hodges–Lehmann estimates comparing DAG-aware generation and vanilla TabPFN, both using topological ordering, in CMD (left) and kMTVD ($k = 2$, right). Positive values indicate that DAG-aware generation achieves lower metric values (i.e., better synthetic data quality). Filled markers with solid error bars indicate significance at $p < 0.05$ (Holm correction).

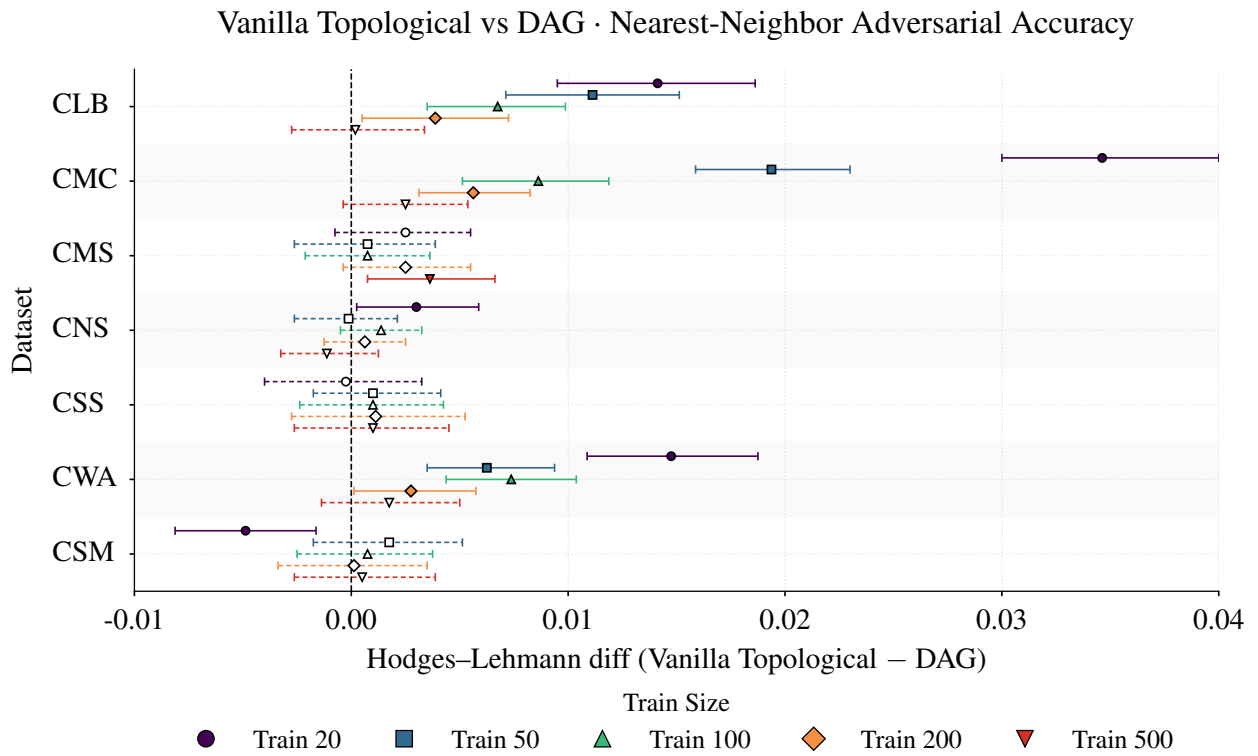


Figure A7: Hodges–Lehmann estimates comparing DAG-aware generation and vanilla TabPFN, both using topological ordering, in NNAA. Positive values indicate that DAG-aware generation achieves lower metric values (i.e., better synthetic data quality). Filled markers with solid error bars indicate significance at $p < 0.05$ (Holm correction).

low accuracy. Figure A10 reports NNAA results. In NNAA, minimal CPDAG shows 19 improvements with no degradations; discovered CPDAG shows no improvements and 4 degradations.

Table A2 reports graph discovery quality for the PC-stable algorithm. Direction recall does not exceed 0.32 across all datasets and training sizes. On most datasets, PC leaves the majority of edges undirected, causing the hybrid strategy to fall back to vanilla conditioning. On CMC, PC orients up to 86 % of discovered edges, but direction precision drops to 0.19 at $N = 500$, leading the strategy to condition on incorrect parents and producing the degradations observed in the main results.

Table A2: PC-stable graph discovery quality on CSuite datasets and the custom SCM, averaged over 100 repetitions. Skeleton recall measures the fraction of true edges recovered. Direction recall measures the fraction of true edge orientations correctly identified. Oriented fraction reports the proportion of discovered edges that PC orients. Direction precision measures the fraction of oriented edges with correct orientation (– indicates no oriented edges).

Dataset	N	Skel. rec.	Dir. rec.	Orient. frac.	Dir. prec.
CSM	20	0.66	0.00	0.02	0.00
	50	0.68	0.00	0.05	0.00
	100	0.68	0.00	0.03	0.00
	200	0.69	0.00	0.06	0.00
	500	0.68	0.00	0.03	0.00
CLB	20	0.08	0.00	0.01	0.00
	50	0.11	0.00	0.05	0.00
	100	0.11	0.00	0.11	0.02
	200	0.12	0.00	0.18	0.01
	500	0.11	0.00	0.19	0.01
CMC	20	0.08	0.01	0.15	0.60
	50	0.19	0.07	0.42	0.63
	100	0.28	0.07	0.56	0.31
	200	0.34	0.09	0.72	0.25
	500	0.40	0.11	0.86	0.19
CMS	20	0.33	0.00	0.01	0.50
	50	0.56	0.01	0.03	0.75
	100	0.59	0.06	0.13	0.81
	200	0.67	0.14	0.25	0.89
	500	0.81	0.32	0.52	0.67
CNS	20	0.24	0.00	0.00	–
	50	0.26	0.00	0.03	0.00
	100	0.28	0.00	0.06	0.04
	200	0.29	0.00	0.07	0.00
	500	0.44	0.00	0.00	–
CSS	20	0.16	0.00	0.00	–
	50	0.30	0.00	0.04	0.00
	100	0.31	0.00	0.01	0.00
	200	0.33	0.00	0.00	–
	500	0.56	0.02	0.05	0.40
CWA	20	0.05	0.00	0.00	–
	50	0.24	0.01	0.10	0.36
	100	0.33	0.01	0.06	0.43
	200	0.38	0.02	0.12	0.35
	500	0.40	0.07	0.23	0.48

I VANILLA TABPFN WITH TOPOLOGICAL ORDERING RESULTS ON ATE PRESERVATION: SGL

Figure A11 reports ATE preservation results for vanilla TabPFN with topological ordering on SGL. Topological ordering produces 5 significant improvements out of 6 training sizes, with larger effect sizes than the CSuite datasets (Figure 3).

Vanilla Original vs Discovered CPDAG · Correlation Matrix Difference

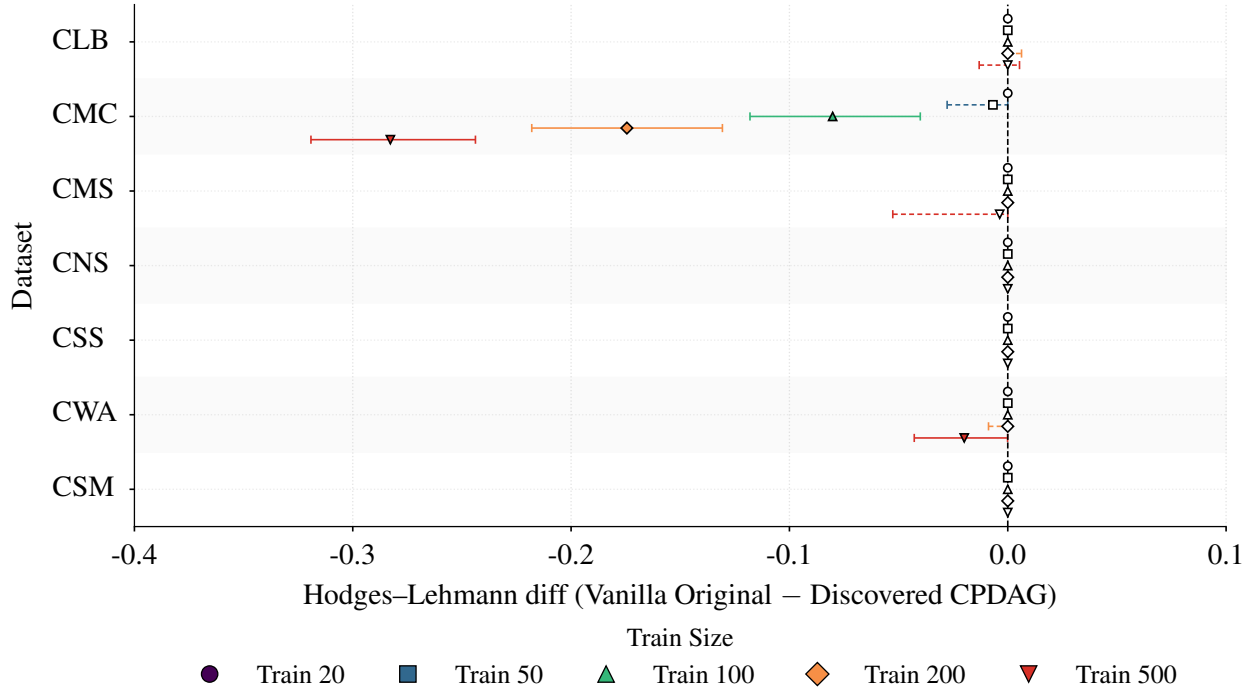


Figure A8: Hodges-Lehmann estimates comparing discovered CPDAG-based generation and vanilla TabPFN with original ordering in CMD. Positive values indicate that CPDAG-based generation achieves lower metric values (i.e., better synthetic data quality). Filled markers with solid error bars indicate significance at $p < 0.05$ (Holm correction).

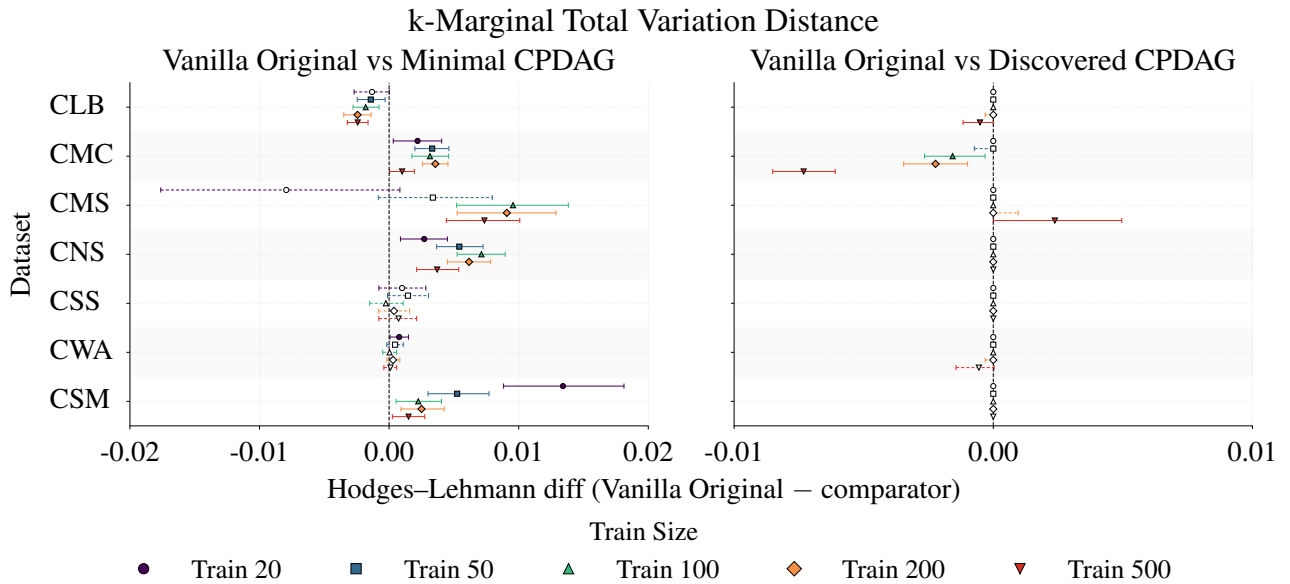


Figure A9: Hodges-Lehmann estimates comparing CPDAG-based generation and vanilla TabPFN with original ordering in kMTVD ($k = 2$), with minimal CPDAG (left) and discovered CPDAG (right). Positive values indicate that CPDAG-based generation achieves lower metric values (i.e., better synthetic data quality). Filled markers with solid error bars indicate significance at $p < 0.05$ (Holm correction).

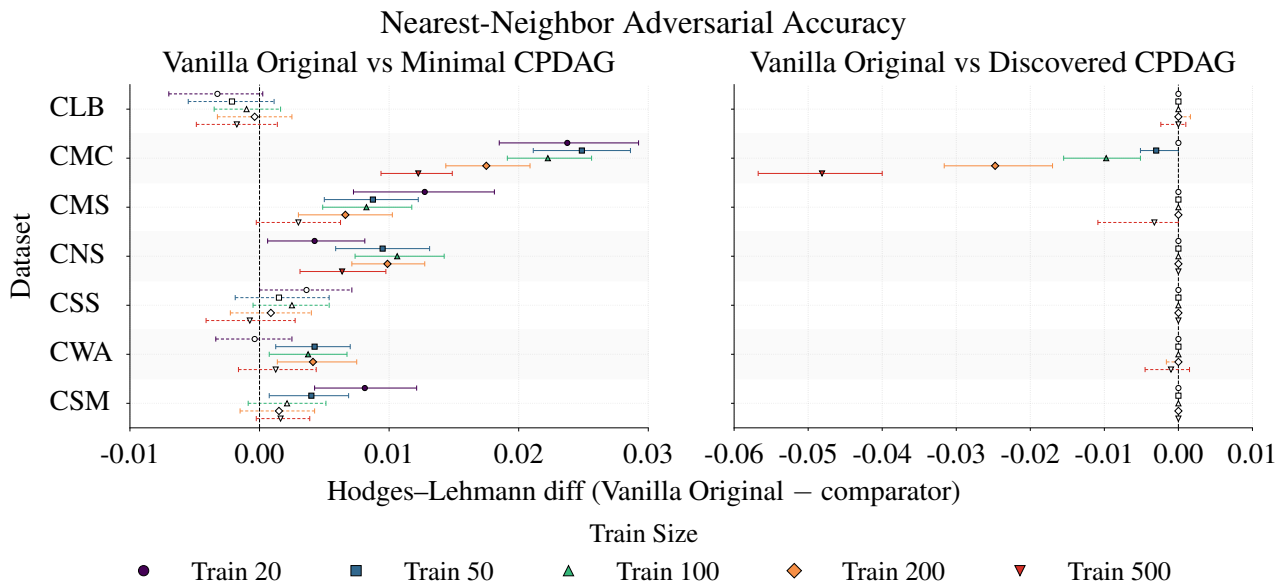


Figure A10: Hodges–Lehmann estimates comparing CPDAG-based generation and vanilla TabPFN with original ordering in NNAA, with minimal CPDAG (left) and discovered CPDAG (right). Positive values indicate that CPDAG-based generation achieves lower metric values (i.e., better synthetic data quality). Filled markers with solid error bars indicate significance at $p < 0.05$ (Holm correction).

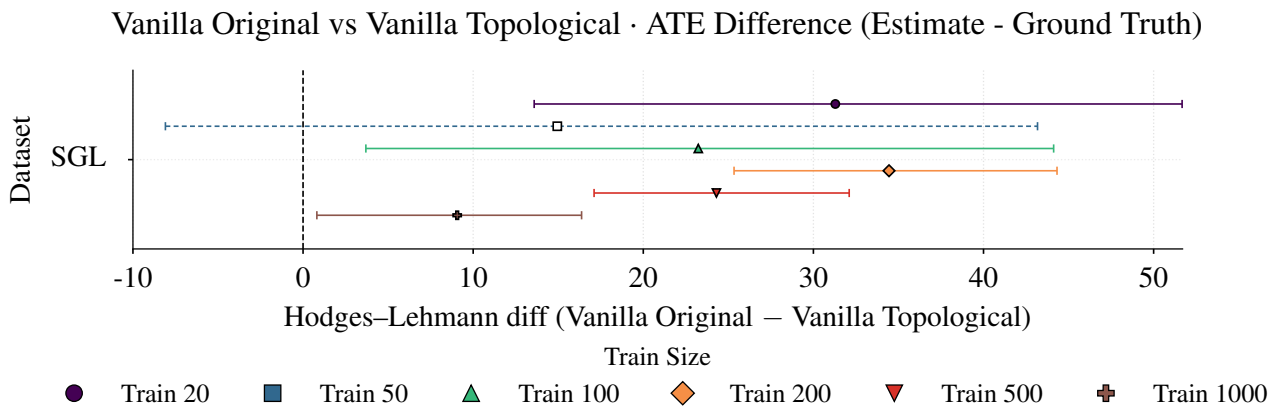


Figure A11: Hodges–Lehmann estimates of the reduction in absolute ATE error (Δ_{ATE}) when comparing vanilla TabPFN with original ordering versus topological ordering on SGL. Positive values indicate that topological ordering produces smaller errors (closer to ground truth), while negative values indicate larger errors. Filled markers indicate significance at $p < 0.05$ (Holm correction).

J VANILLA TABPFN WITH REVERSE TOPOLOGICAL ORDERING RESULTS ON ATE PRESERVATION

Figure A12 reports results for reverse topological ordering. Reverse topological ordering shows 8 significant improvements and 7 degradations. The largest degradation occurs on CSM at 20 samples.

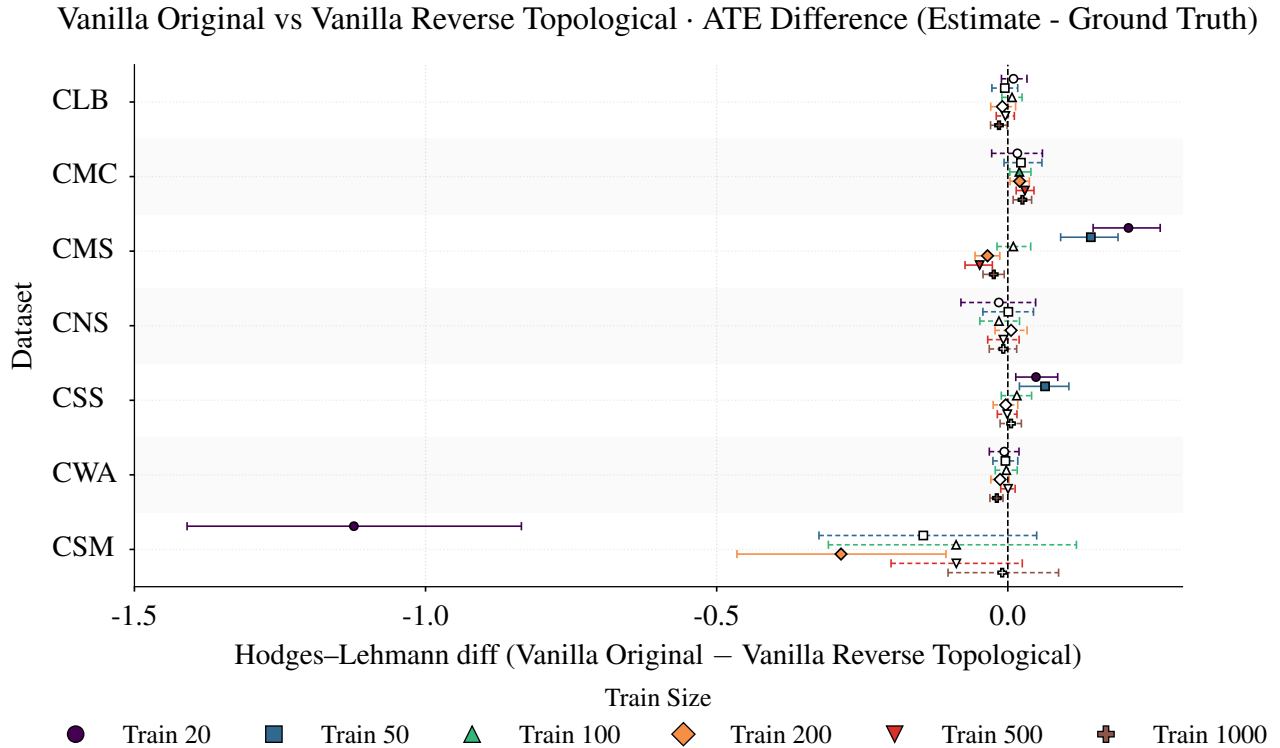


Figure A12: Hodges–Lehmann estimates of the reduction in absolute ATE error (Δ_{ATE}) when comparing vanilla TabPFN with original ordering versus reverse topological ordering on ATE preservation. Positive values indicate that reverse topological ordering produces smaller errors (closer to ground truth), while negative values indicate larger errors. Filled markers with solid error bars indicate significance at $p < 0.05$ (Holm correction).

K DAG-AWARE GENERATION WITH TOPOLOGICAL ORDERING ON ATE PRESERVATION

We compare DAG-aware generation and vanilla TabPFN when both use topological ordering, isolating the contribution of causal parent-based conditioning from the feature ordering itself.

DAG-aware generation shows 15 significant improvements with no degradations (Figure A13). CSM shows significant improvements across most training sizes, confirming that causal parent conditioning provides benefits beyond feature ordering alone.

L DISCOVERED CPDAG RESULTS ON ATE PRESERVATION

Figure A14 reports ATE preservation results for discovered CPDAG. The discovered CPDAG shows one significant improvement on CMC at $N = 1000$ and one degradation on CWA at $N = 1000$. Table A3 reports graph discovery quality against the mutilated DAG (the causal graph with edges into the treatment variable removed), which is the appropriate reference for interventional data. On CMC at $N = 1000$, PC orients 88% of discovered edges with direction precision

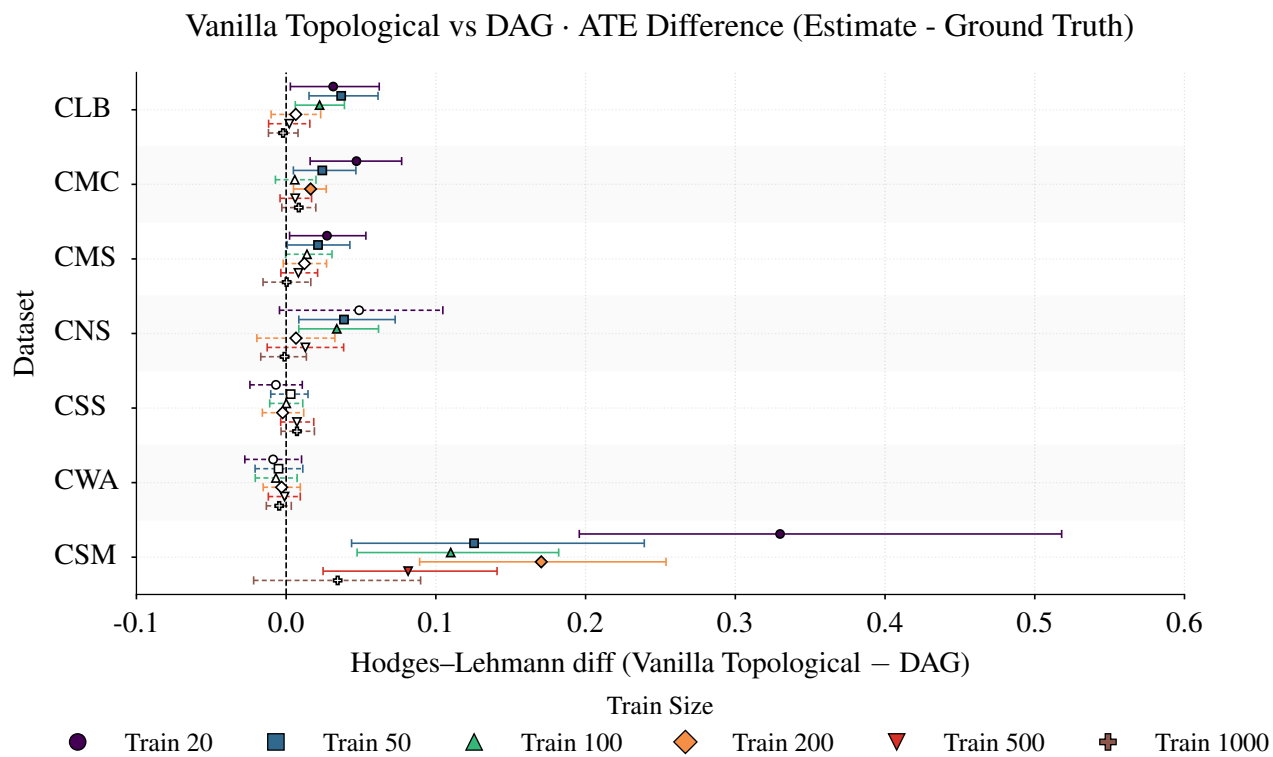


Figure A13: Hodges–Lehmann estimates of the reduction in absolute ATE error (Δ_{ATE}) when comparing vanilla TabPFN with topological ordering versus DAG-aware generation. Positive values indicate that DAG-aware generation produces smaller errors (closer to ground truth). Filled markers with solid error bars indicate significance at $p < 0.05$ (Holm correction).

0.24, providing enough correct structure around the treatment–outcome path to improve ATE estimation. On CWA at $N = 1000$, PC orients only 28% of edges with direction precision 0.02, causing the few oriented edges to introduce incorrect conditioning around the treatment–outcome relationship.

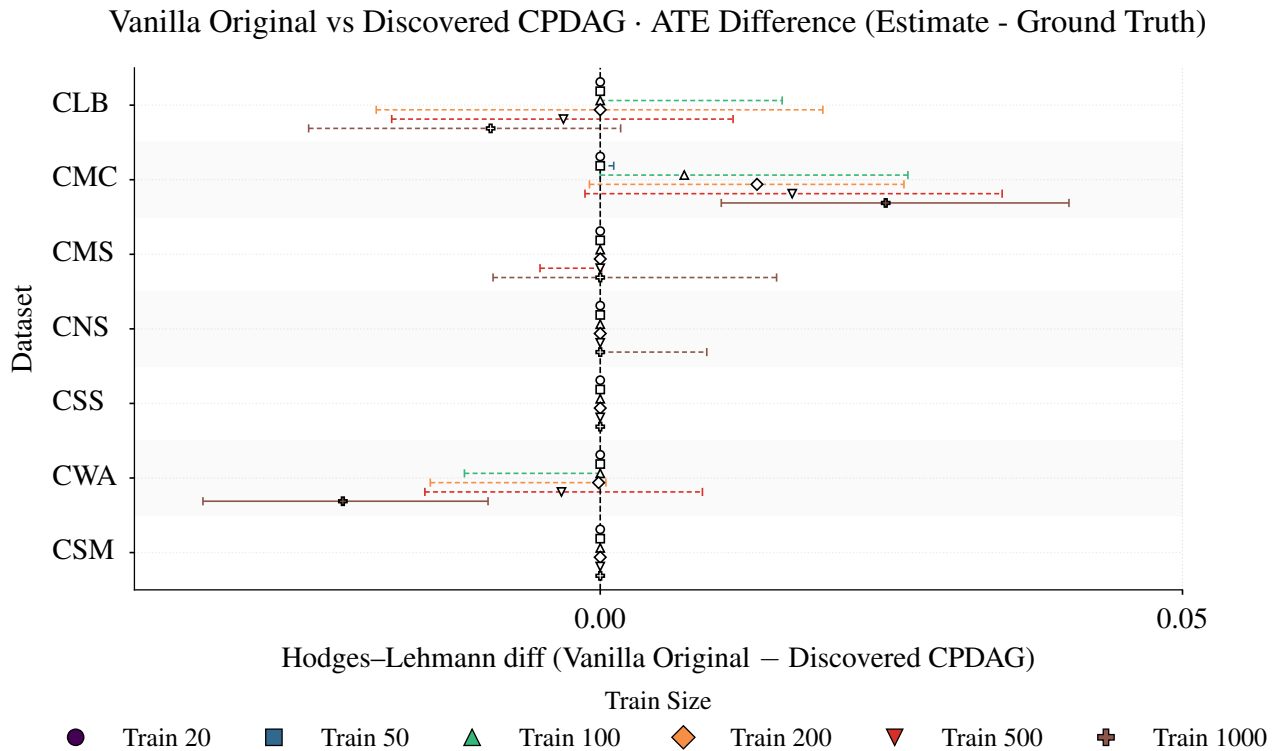


Figure A14: Hodges–Lehmann estimates of the reduction in absolute ATE error (Δ_{ATE}) when comparing vanilla TabPFN with original ordering versus discovered CPDAG on ATE preservation. Positive values indicate that discovered CPDAG produces smaller errors (closer to ground truth), while negative values indicate larger errors. Filled markers with solid error bars indicate significance at $p < 0.05$ (Holm correction).

M ROBUSTNESS TO HIGHER NOISE

To verify that the findings reported in the main text are not specific to the near-deterministic regime ($\sigma = 10^{-5}$), we repeat the synthetic data quality experiments on the custom SCM with $\sigma = 10^{-2}$ (denoted CSMn2 in the figures).

DAG-aware generation shows significant improvements over vanilla TabPFN across all training sizes in both CMD and kMTVD (Figure A15). In NNAA, improvements are significant at $N \in \{20, 50\}$ but not at larger training sizes (Figure A16), consistent with the $\sigma = 10^{-5}$ results.

Minimal CPDAG shows the same pattern: significant improvements in CMD and kMTVD across all training sizes (Figures A17 and A18), with NNAA significant only at small N (Figure A19). Discovered CPDAG shows no meaningful differences across metrics and training sizes, consistent with the $\sigma = 10^{-5}$ results.

These results confirm that the benefits of causal conditioning extend beyond the near-deterministic regime.

Table A4 confirms that spurious correlations under $\sigma = 10^{-2}$ are comparable in magnitude to those observed under $\sigma = 10^{-5}$ (Table A1). Minimal CPDAG shows reduced correlations under higher noise, suggesting increased robustness to imprecise conditioning from undirected edges.

Table A3: PC-stable graph discovery quality on CSuite datasets and the custom SCM for the ATE experiments, averaged over 100 repetitions. Metrics are computed against the mutilated DAG (edges into the treatment variable removed). Skeleton recall measures the fraction of true edges recovered. Direction recall measures the fraction of true edge orientations correctly identified. Oriented fraction reports the proportion of discovered edges that PC orients. Direction precision measures the fraction of oriented edges with correct orientation (– indicates no oriented edges).

Dataset	N	Skel. rec.	Dir. rec.	Orient. frac.	Dir. prec.
CSM	20	0.68	0.00	0.03	0.00
	50	0.68	0.00	0.05	0.00
	100	0.68	0.00	0.03	0.00
	200	0.67	0.00	0.01	0.00
	500	0.67	0.00	0.01	0.00
	1000	0.67	0.00	0.00	–
CLB	20	0.19	0.00	0.01	0.50
	50	0.53	0.01	0.08	0.29
	100	0.78	0.05	0.24	0.21
	200	0.91	0.04	0.28	0.13
	500	1.00	0.04	0.32	0.07
	1000	1.00	0.03	0.31	0.03
CMC	20	0.07	0.01	0.17	0.30
	50	0.18	0.08	0.39	0.65
	100	0.22	0.11	0.60	0.52
	200	0.24	0.14	0.75	0.44
	500	0.33	0.18	0.81	0.39
	1000	0.38	0.15	0.88	0.24
CMS	20	0.27	0.01	0.19	0.20
	50	0.43	0.02	0.14	0.23
	100	0.46	0.01	0.14	0.14
	200	0.64	0.02	0.38	0.07
	500	0.82	0.02	0.61	0.04
	1000	0.88	0.03	0.71	0.03
CNS	20	0.31	0.00	0.02	0.50
	50	0.40	0.00	0.00	–
	100	0.56	0.00	0.06	0.12
	200	0.64	0.01	0.10	0.14
	500	0.71	0.00	0.20	0.00
	1000	0.83	0.00	0.59	0.00
CSS	20	0.38	0.01	0.05	0.67
	50	0.50	0.09	0.17	1.00
	100	0.67	0.06	0.12	0.75
	200	0.67	0.00	0.02	0.00
	500	0.67	0.00	0.00	–
	1000	0.67	0.00	0.01	0.00
CWA	20	0.14	0.01	0.10	0.40
	50	0.43	0.02	0.14	0.31
	100	0.50	0.01	0.15	0.12
	200	0.53	0.01	0.19	0.11
	500	0.58	0.01	0.29	0.02
	1000	0.58	0.01	0.28	0.02

Table A4: Mean Pearson correlation coefficients for independent variable pairs in the custom collider SCM with $\sigma = 10^{-2}$. Values close to zero indicate correct independence preservation. Standard deviations across 100 repetitions in parentheses.

Method	$\rho(X_0, X_3)$	$\rho(X_0, X_2)$
<i>Train size N = 20</i>		
Vanilla original	-0.147 (0.205)	-0.145 (0.206)
Vanilla topological	-0.015 (0.116)	-0.014 (0.115)
Vanilla reverse top.	-0.121 (0.202)	-0.119 (0.204)
DAG-aware	0.004 (0.021)	0.003 (0.021)
Minimal CPDAG	0.003 (0.023)	0.004 (0.021)
Discovered CPDAG	-0.136 (0.215)	-0.134 (0.216)
<i>Train size N = 100</i>		
Vanilla original	-0.043 (0.113)	-0.043 (0.113)
Vanilla topological	-0.017 (0.064)	-0.017 (0.063)
Vanilla reverse top.	-0.049 (0.102)	-0.047 (0.102)
DAG-aware	0.000 (0.020)	0.001 (0.020)
Minimal CPDAG	-0.002 (0.025)	0.000 (0.020)
Discovered CPDAG	-0.022 (0.143)	-0.022 (0.145)
<i>Train size N = 500</i>		
Vanilla original	-0.027 (0.043)	-0.027 (0.042)
Vanilla topological	-0.004 (0.025)	-0.003 (0.025)
Vanilla reverse top.	-0.033 (0.039)	-0.032 (0.039)
DAG-aware	0.000 (0.023)	0.001 (0.023)
Minimal CPDAG	0.000 (0.023)	0.000 (0.023)
Discovered CPDAG	0.016 (0.146)	0.019 (0.155)
Test set	0.022 -	0.022 -

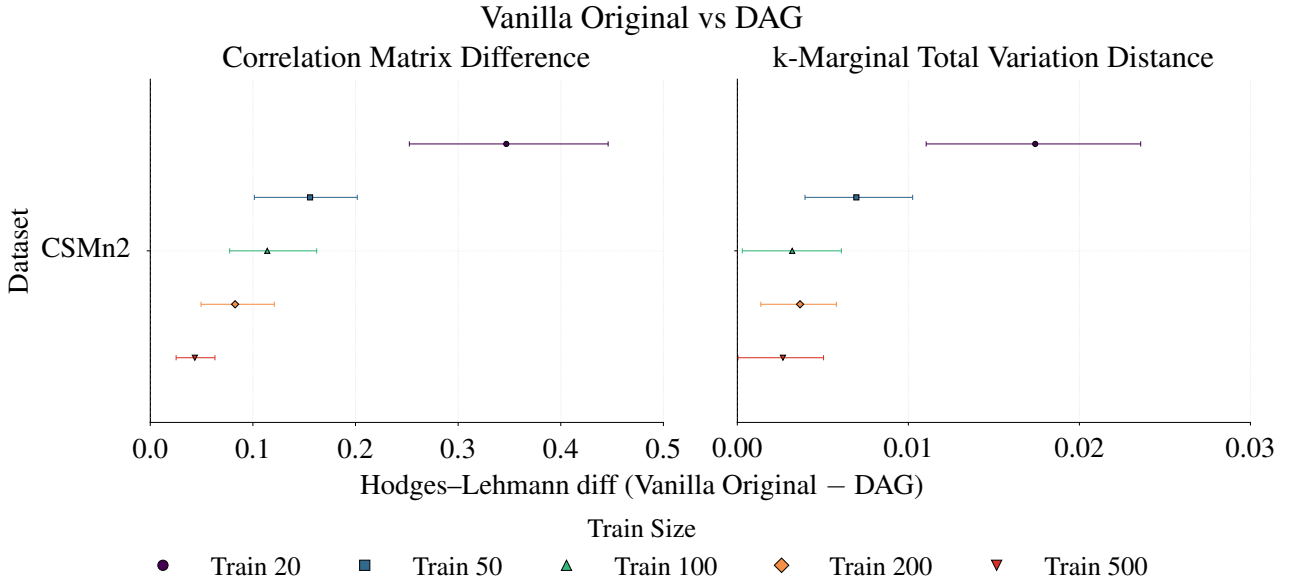


Figure A15: Hodges–Lehmann estimates comparing DAG-aware generation and vanilla TabPFN with original ordering on the custom SCM with $\sigma = 10^{-2}$, in CMD (left) and kMTVD ($k = 2$, right). Positive values indicate that DAG-aware generation achieves lower metric values (i.e., better synthetic data quality). Filled markers with solid error bars indicate significance at $p < 0.05$ (Holm correction).

Vanilla Original vs DAG · Nearest-Neighbor Adversarial Accuracy

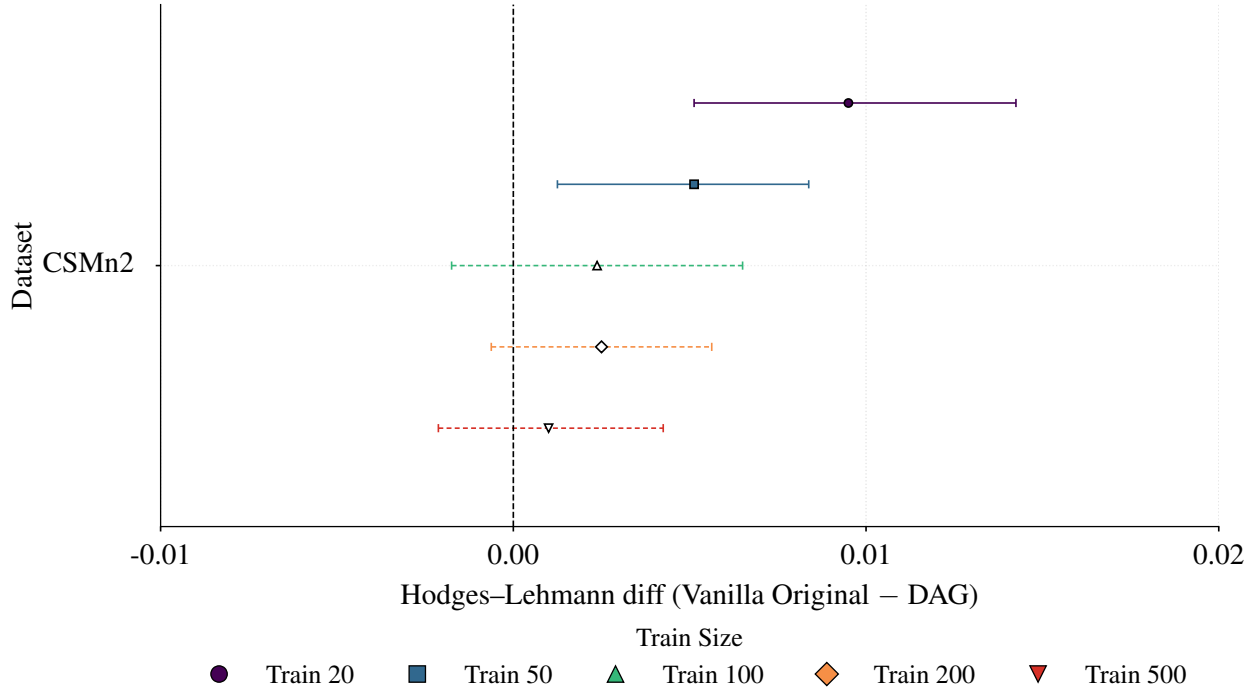


Figure A16: Hodges–Lehmann estimates comparing DAG-aware generation and vanilla TabPFN on the custom SCM with $\sigma = 10^{-2}$, in NNA. Positive values indicate that DAG-aware generation achieves lower metric values (i.e., better synthetic data quality). Filled markers with solid error bars indicate significance at $p < 0.05$ (Holm correction).

Correlation Matrix Difference

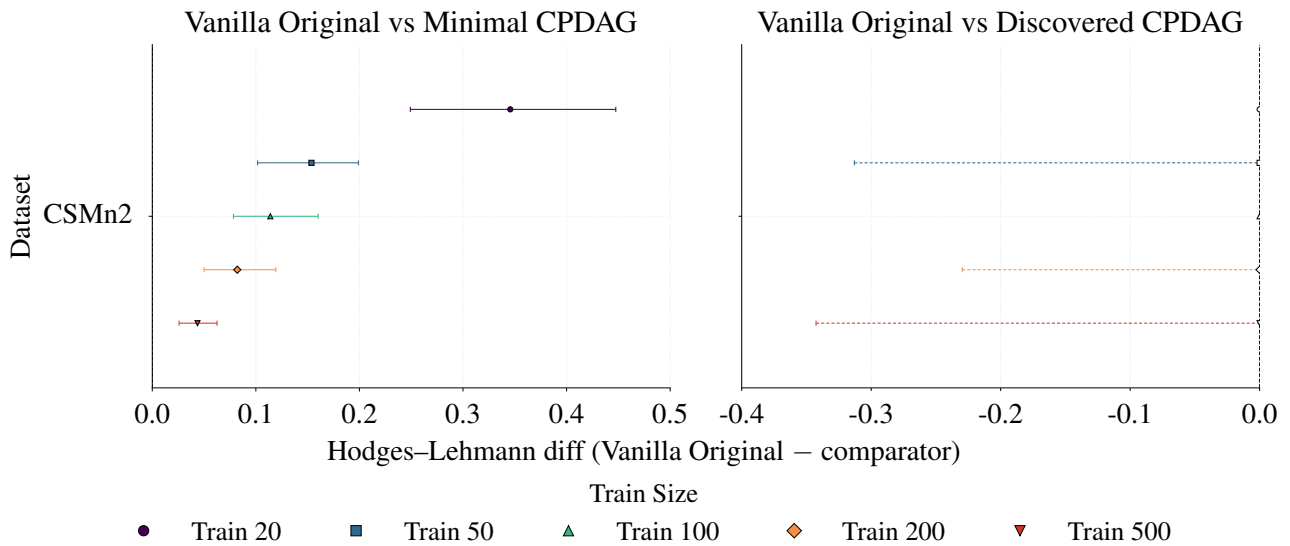


Figure A17: Hodges–Lehmann estimates comparing CPDAG-based generation and vanilla TabPFN on the custom SCM with $\sigma = 10^{-2}$, in CMD, with minimal CPDAG (left) and discovered CPDAG (right). Positive values indicate that CPDAG-based generation achieves lower metric values (i.e., better synthetic data quality). Filled markers with solid error bars indicate significance at $p < 0.05$ (Holm correction).

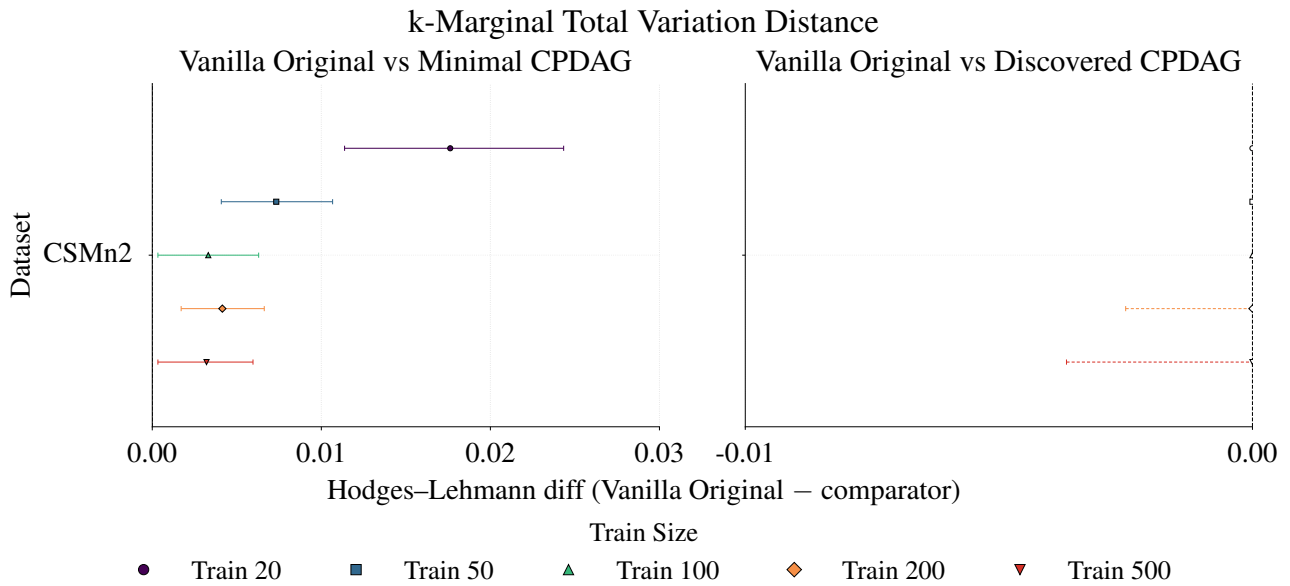


Figure A18: Hodges–Lehmann estimates comparing CPDAG-based generation and vanilla TabPFN with original ordering on the custom SCM with $\sigma = 10^{-2}$, in kMTVD ($k = 2$), with minimal CPDAG (left) and discovered CPDAG (right). Positive values indicate that CPDAG-based generation achieves lower metric values (i.e., better synthetic data quality). Filled markers with solid error bars indicate significance at $p < 0.05$ (Holm correction).

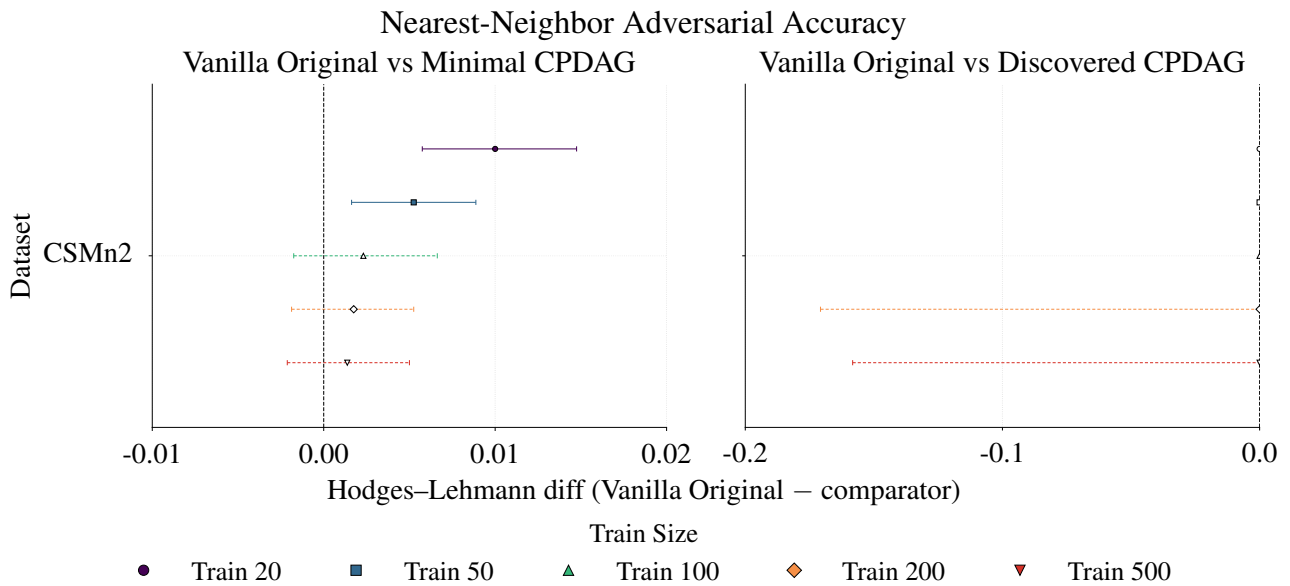


Figure A19: Hodges–Lehmann estimates comparing CPDAG-based generation and vanilla TabPFN on the custom SCM with $\sigma = 10^{-2}$, in NNAA, with minimal CPDAG (left) and discovered CPDAG (right). Positive values indicate that CPDAG-based generation achieves lower metric values (i.e., better synthetic data quality). Filled markers with solid error bars indicate significance at $p < 0.05$ (Holm correction).

TREATMENT EFFECT PRESERVATION

DAG-aware generation significantly improves ATE preservation across $N \in \{20, 50, 100, 200, 500\}$ compared to vanilla TabPFN (Figure A20). At $N = 1000$, the direction remains favorable but not statistically significant. Minimal CPDAG shows the same pattern (Figure A21). Discovered CPDAG shows no differences across training sizes.

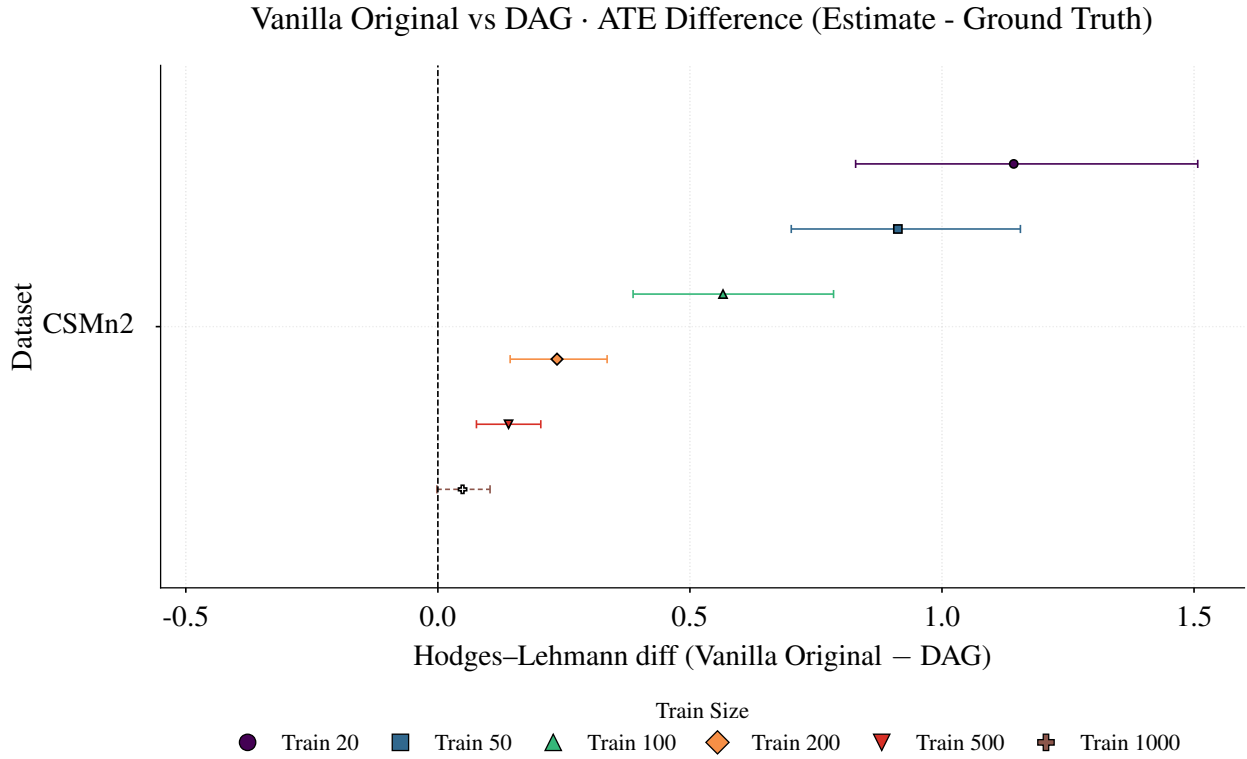


Figure A20: Hodges–Lehmann estimates of the reduction in absolute ATE error (Δ_{ATE}) when comparing vanilla TabPFN with original ordering versus DAG-aware generation on the custom SCM with $\sigma = 10^{-2}$. Positive values indicate that the DAG-aware generation produces smaller errors (closer to ground truth), while negative values indicate larger errors. Filled markers with solid error bars indicate significance at $p < 0.05$ (Holm correction).

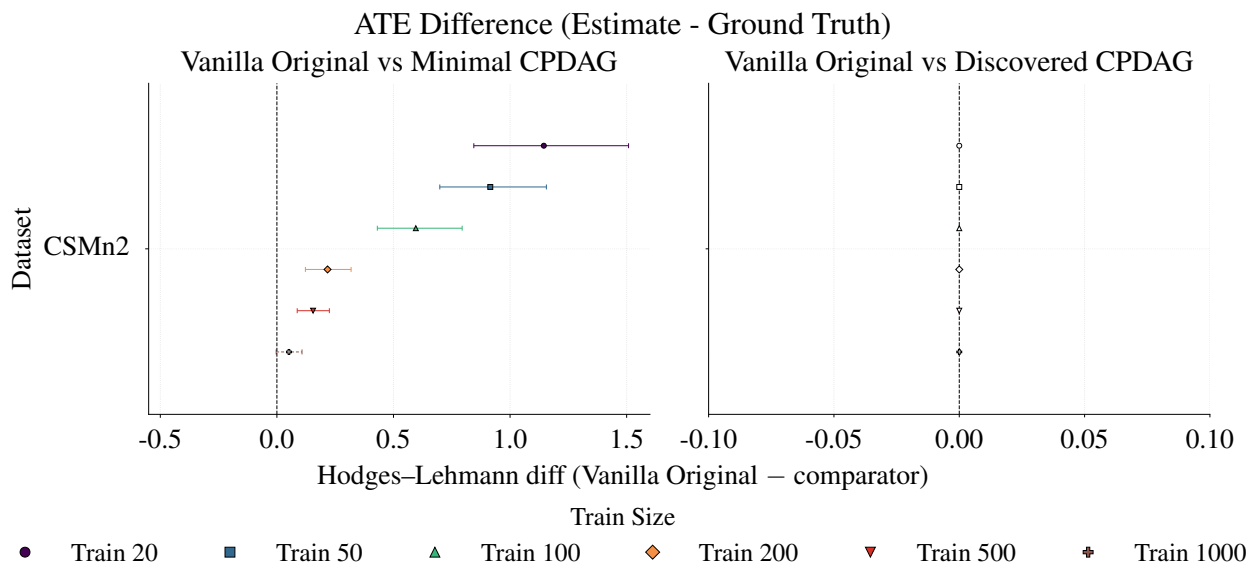


Figure A21: Hodges–Lehmann estimates of the reduction in absolute ATE error (Δ_{ATE}) when comparing vanilla TabPFN with original ordering versus CPDAG-based generation on the custom SCM with $\sigma = 10^{-2}$, with minimal CPDAG (left) and discovered CPDAG (right). Positive values indicate that the respective method (minimal CPDAG or discovered CPDAG) produces smaller errors (closer to ground truth), while negative values indicate larger errors. Filled markers with solid error bars indicate significance at $p < 0.05$ (Holm correction).

N CAUSAL DISCOVERY WITH REX

To assess the sensitivity of our approach to the choice of causal discovery algorithm, we tested REX [Renero et al., 2026], a method that employs machine learning regressors for skeleton discovery and exploits additive noise model assumptions to orient edges, on the four CSuite datasets that satisfy this assumption (CLB, CNS, CSS, CWA). We ran REX with default hyperparameters, as preliminary tests showed no meaningful difference with tuning at these sample sizes. Given the consistent degradations observed across all distributional metrics, we did not extend the evaluation to ATE preservation.

Table A5 reports graph quality metrics averaged over 100 repetitions. REX exhibits low direction precision at small and medium training sizes, particularly on CLB, CNS, and CWA (below 50% for $N \leq 100$). Graph quality improves at $N = 500$ for CLB (0.95 skeleton recall, 0.95 direction precision) and CSS (1.00 direction precision, 0.61 recall). CNS achieves high direction precision at $N = 500$ but skeleton recall remains at 0.50. CWA maintains 0.75 direction precision and 0.57 recall even at $N = 500$.

Using REX-discovered DAGs for causal conditioning leads to significant degradations compared to vanilla TabPFN across nearly all dataset–training size combinations: 15 significant degradations with no significant improvements in CMD, and 19 significant degradations with no improvements in both kMTVD and NNAA (Figures A22 and A23).

These results confirm that the quality of the discovered causal graph is critical: incorrect graphs actively harm synthetic data quality. This motivates the use of conservative algorithms such as PC combined with our hybrid conditioning strategy, which falls back to vanilla sequential generation for undirected edges rather than committing to potentially wrong directions.

Table A5: REX graph quality on CSuite datasets, averaged over 100 repetitions. Since REX returns fully oriented DAGs, all discovered edges are directed. Skeleton recall measures the fraction of true edges recovered. Direction precision measures the fraction of oriented edges with correct orientation.

Dataset	N	Skel. recall	Dir. prec.
CLB	20	0.70	0.48
	50	0.73	0.45
	100	0.86	0.47
	200	0.91	0.62
	500	0.95	0.95
CNS	20	0.57	0.37
	50	0.53	0.36
	100	0.51	0.32
	200	0.51	0.70
	500	0.50	0.99
CSS	20	0.51	0.57
	50	0.47	0.64
	100	0.51	0.88
	200	0.62	0.99
	500	0.61	1.00
CWA	20	0.56	0.44
	50	0.55	0.41
	100	0.62	0.39
	200	0.58	0.50
	500	0.57	0.75

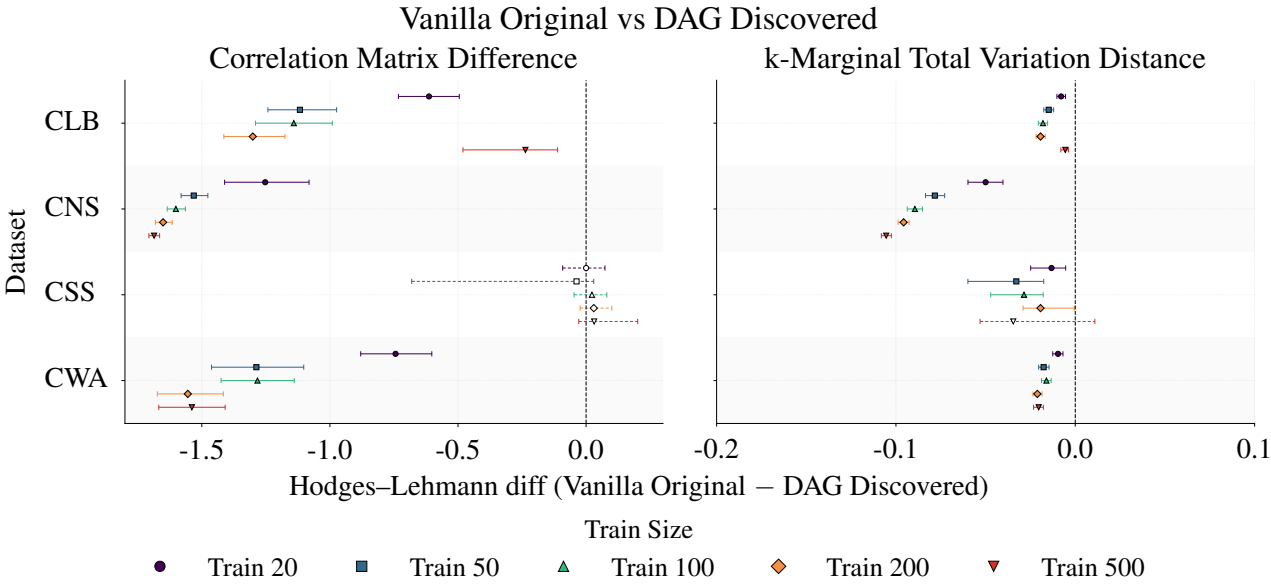


Figure A22: Hodges-Lehmann estimates comparing DAG-aware generation with REX-discovered graphs and vanilla TabPFN with original ordering, in CMD (left) and kMTVD ($k = 2$, right). Positive values indicate that the REX-based approach achieves lower metric values (i.e., better synthetic data quality). Filled markers with solid error bars indicate significance at $p < 0.05$ (Holm correction).

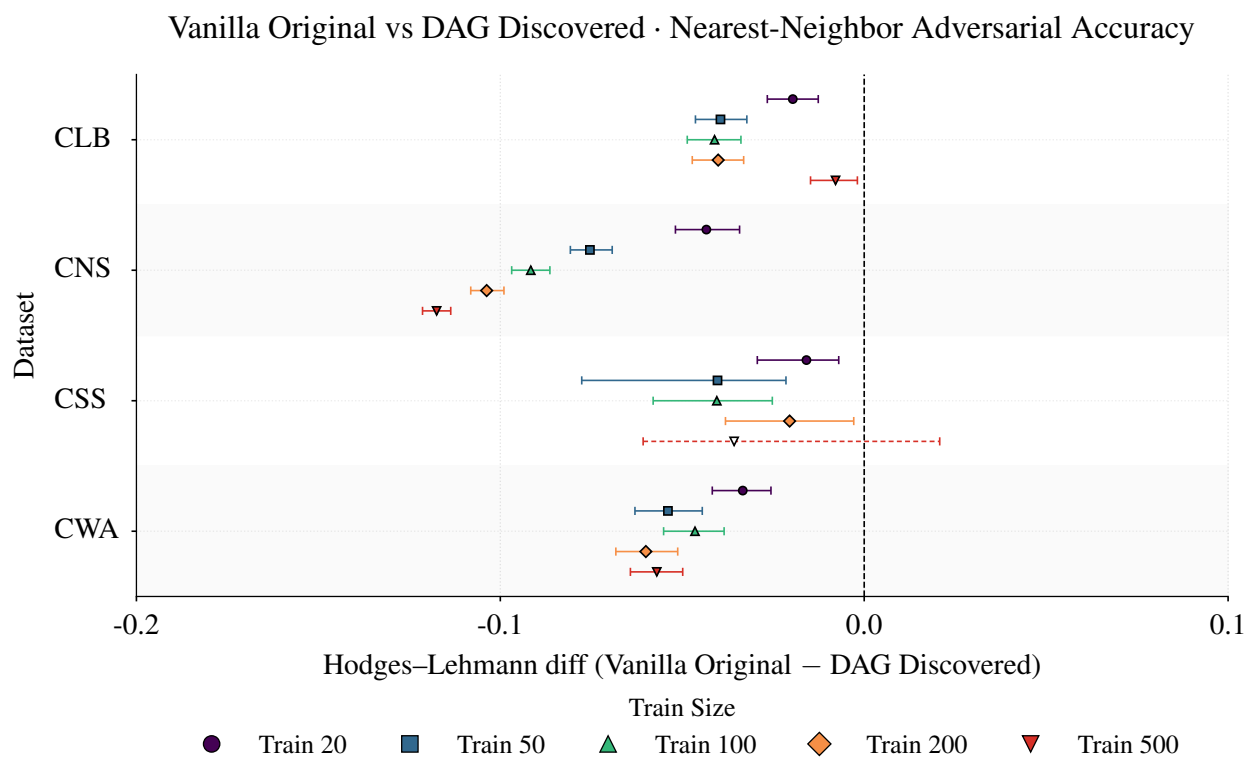


Figure A23: Hodges–Lehmann estimates comparing DAG-aware generation with REX-discovered graphs and vanilla TabPFN with original ordering, in NNAA. Positive values indicate that the REX-based approach achieves lower metric values (i.e., better synthetic data quality). Filled markers with solid error bars indicate significance at $p < 0.05$ (Holm correction).